



**NTNU – Trondheim**  
Norwegian University of  
Science and Technology

# Development of a low drag suit for sprint races

**Camilla Fydrych Sæter**

Master of Energy Use and Energy Planning

Submission date: June 2013

Supervisor: Lars Sætran, EPT

Co-supervisor: Luca Oggiano, EPT  
Lars Morten Bardal, EPT

Norwegian University of Science and Technology  
Department of Energy and Process Engineering



EPT-M-2013-114

**MASTER THESIS**

for

stud.tech. Camilla Fydrych Sæter

Spring 2013

**On using textiles to influence the drag-force of bluff bodies***Bruk av tekstiler til å endre motstandskraften for butte legemer***Background**

The advantage of tripping the turbulent flow around bluff bodies with rough surfaces in order to be able to reduce the drag and stabilize the flow has been known for many decades and applied in a number of engineering fields. In 2002 NIKE developed the swift suit for speed skating competition. The suit was designed with a patched design where each body part was covered with a different fabric forcing the transition to turbulent regime at the wanted speed and thus dramatically reducing the drag. From 2002, the interest in low drag suits has been rapidly growing and their applications extended from speed skating to other sports such as cycling, skiing and running.

The present master thesis will focus on a new model of low drag suit for sprint competitions currently under development at Adidas, aiming to test it and improve it.

The work will consist in both dynamic and static measurements carried out on oval and tapered cylindrical models and on a full scale mannequin. Both the suit fabric and a manipulated under-layer should be tested and relationships between cylindrical models and legs are suggested to be established.

Tests will be carried out in the wind tunnel at NTNU using a high frequency force plate (AMTI BP-600400HF).

-- " --

Within 14 days of receiving the written text on the master thesis, the candidate shall submit a research plan for his project to the department.

When the thesis is evaluated, emphasis is put on processing of the results, and that they are presented in tabular and/or graphic form in a clear manner, and that they are analyzed carefully.

The thesis should be formulated as a research report with summary both in English and Norwegian, conclusion, literature references, table of contents etc. During the preparation of the text, the candidate should make an effort to produce a well-structured and easily readable report. In order to ease the evaluation of the thesis, it is important that the cross-references are correct. In the making of the report, strong emphasis should be placed on both a thorough discussion of the results and an orderly presentation.

The candidate is requested to initiate and keep close contact with his/her academic supervisor(s) throughout the working period. The candidate must follow the rules and regulations of NTNU as well as passive directions given by the Department of Energy and Process Engineering.

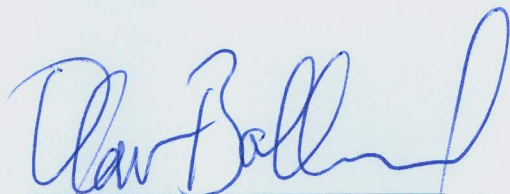
Risk assessment of the candidate's work shall be carried out according to the department's procedures. The risk assessment must be documented and included as part of the final report. Events related to the candidate's work adversely affecting the health, safety or security, must be documented and included as part of the final report. If the documentation on risk assessment represents a large number of pages, the full version is to be submitted electronically to the supervisor and an excerpt is included in the report.

Pursuant to "Regulations concerning the supplementary provisions to the technology study program/Master of Science" at NTNU §20, the Department reserves the permission to utilize all the results and data for teaching and research purposes as well as in future publications.

The final report is to be submitted digitally in DAIM. An executive summary of the thesis including title, student's name, supervisor's name, year, department name, and NTNU's logo and name, shall be submitted to the department as a separate pdf file. Based on an agreement with the supervisor, the final report and other material and documents may be given to the supervisor in digital format.

- Work to be done in lab (Water power lab, Fluids engineering lab, Thermal engineering lab)  
 Field work

Department of Energy and Process Engineering, 14. January 2013



Olav Bolland  
Department Head



Lars Sætran  
Academic Supervisor

Co-Supervisors: Dr Luca Oggiano, Lars M Bardal

# Development of a low drag suit for sprint races

Camilla Fydrych Sæter  
Norwegian University of Science and Technology  
Department of Energy and Process Engineering

## Abstract—

The present master thesis given in this paper is a follow up of the project thesis presented by the writing author and it aims to design a custom suit to reduce the drag on a 100m sprinter. Knowing that different surface roughness is able to modify the flow field around a bluff body, different types of surface roughness will be analyzed. These different surfaces are obtained combining an under layer made with rubber strips with a top layer. Tests have been conducted in the wind tunnel on different models (oval cylinders, tapered cylinders, circular cylinders and full scale mannequin) were carried out in order to establish the right combination of under layer and top layer. Additional tests to evaluate how different accelerations affect the drag crisis were conducted and a hysteresis phenomenon in the drag crisis process was found and investigated. A force plate with a high natural frequency (470Hz) was utilized to measure the aerodynamic drag force. The results show that it is possible to trigger early transition causing at drag crisis at Reynolds number that match the athlete's speeds during a sprinting race (<15m/s). This can be obtained using the right combination of strips and top layer. Shape, size, angle of attack and yaw angle were proven not to play a major role in the drag crisis process. A custom underlayer for an existing suit has been designed and proved to reduce the overall aerodynamic drag when compared with the existing suits provided by Adidas.

## I. INTRODUCTION

In short distance sprinting races like the 100 m or 200 m dash, winning and losing can come down to a fraction of a second. During these races, most of the power output generated by the athletes is used to increase the speed (and thus to overcome the inertial force) and to overcome the aerodynamic drag. Being the drag proportional to the square of the speed, its relative importance is negligible for low speeds but it might play a relevant role when the athletes reach their maximum speed which lays between 10 m/s and 15 m/s[1]

Focusing then on the aerodynamic drag acting against a runner, writing the drag [D] as  $D=0.5\rho U^2 A C_D$  and being the air density  $\rho$  [ $kg/m^3$ ] and the speed  $U$  [ $m/s$ ] typical quantities that depend exclusively on the location and on the performance, the possible adjustments that could be done in order to reduce the drag have to focus either on the frontal area  $A$  [ $m^2$ ] or on the non-dimensional drag coefficient  $C_D$  [-].

The frontal area could be reduced by modifying the running posture of the athlete. However, this kind of adjustments would require a biomechanical study of the running technique in order to be efficient and will therefore not be presented in this work.

The drag coefficient,  $C_D$  depends strongly on the shape, Reynolds number and surface properties of the body and some adjustments can be made. The drag coefficient can be considered as the sum of a skin friction drag coefficient and a pressure drag coefficient  $C_D = C_{Df} + C_{Dp}$ , where the subscript  $f$  indicates the friction drag and the subscript  $p$  indicates pressure drag[2]. The skin friction drag is caused by the viscous friction along the surface of the body while the pressure drag is caused by an asymmetrical pressure distribution on the upstream

and downstream side of the body. Both effects must then be considered when trying to minimize the total drag coefficient,  $C_D$ . It is however well known that the relative contribution from the pressure- and friction drag depends on the object shape. On a bluff body such as an athlete body, the pressure drag contributes the most to the total drag [3]. The friction drag will then be considered negligible and the attention will be focused in triggering turbulent flow on the body surface. The turbulent flow will stay more attached to the body, moving the separation point downstream, reducing the wake size and thus the pressure drag.

***Flow phases:*** the flow around a bluff body can have two different phases. It can be either laminar or turbulent and this division is mostly is governed by the Reynolds number, which depends mainly on the ratio of inertial forces to viscous forces in the fluid and can be defined as  $Re = UD/\nu$ , where where  $U$  is the free-stream velocity,  $D$  is the characteristic length of the model used (e.g. the diameter of a cylinder), and  $\nu$  is the kinematic.

Laminar flow occurs at low Reynolds numbers, where the viscous forces are stronger than the inertial forces. The separate region past the body is however highly turbulent with a wide turbulent wake. When the inertial forces are starting to be dominant, a transitional regime occurs. The transitional phase is often abrupt and it was studied by a number of authors. The transition phase itself is associated with three various regimes and each regime are explained in detail by Zdravkovich[4, 5]. These regimes involve the wake, separated shear layer and boundary layer and each phase occurs at different Reynolds number.

In the transition regime the flow evolves from laminar to turbulent and an abrupt reduction in terms of drag can be observed, this phenomenon is called “drag crisis”. The decrease in drag coefficient,  $C_D$  is due to the flow in the boundary layer becoming turbulent. This process moves the separation point further downstream on the body, reducing the size of the wake and thus the magnitude of the pressure drag.

Once the transition is completed, the flow around the body is fully turbulent. The turbulent regime is

characterized by lower value of  $C_D$  due to the shifting of the separation point towards the back side of the cylinder and thus a smaller wake and a lower pressure drag[4, 5]. A deeper look at the transition phenomenon is hereby given.

***Flow transition:*** The transition phenomenon has mostly been studied on circular cylinders and some authors gave a detailed description of it.

Wieselsberger first [6] used the term subcritical and supercritical to describe the flow states before and after the “drag crisis” (Figure 1). He mentioned that a break in the symmetry with two discontinuous transitions can be often seen during the transitional phase (in cylinders). This is due to the different behaviors of the two sides of the cylinder where transition occurs separately.

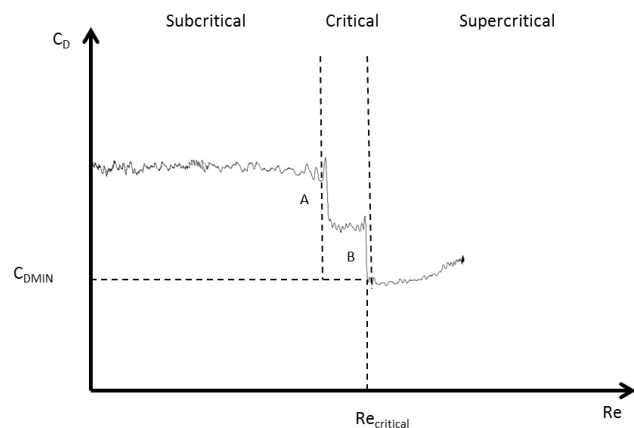


**Figure 1 - Typical  $C_D$  - Reynolds number curve for a cylinder and detailed structure of the critical range, with two discontinuous transitions, A and B**

Schewe and Zdravkovich [4, 7-9] separately explained this behavior saying that the transition from laminar to turbulent flow in the boundary layer occurs first on one side of the cylinder. They called this regime “single bubble regime”. The asymmetric single bubble regime comes to an end at higher Reynolds numbers with yet another discontinues fall in drag coefficient,  $C_D$ . At this stage a second bubble is formed on the other side of the cylinder and this stage is then called “two bubble regime”. The symmetric two bubble regime occurs in the supercritical regime and represents a complicated combination of laminar separation, transition, reattachment and turbulent separation of the boundary layers on both sides of the cylinder. This

discontinuous jumps between individual states can be interpreted as subcritical bifurcations.

The flow transition is a non-linear process and it is extremely sensitive to small disturbances, such as surface roughness, free stream turbulence, speed gradients, non-uniformity of the flow, etc. Being unable to modify the other parameters mentioned the attention will be focused on the surface roughness.

A large number of previous studies confirmed that the introduction of surface roughness on the cylinder surface can shift the transition to a lower critical Reynolds number which results in a drop in terms of  $C_D$ [10-12].

These results and studies pushed the research on sports garment aerodynamic and led to the design of low drag suits where the suits are made with different patches each of them characterized by a different surface roughness. The first low drag suit was developed by NIKE which introduced its “NIKE swift suit” in 2002[13] after this success the focus of sports companies on low drag skin suits suddenly increased. This suit was developed from previous studies carried out by Brownlie [14]. In his work Brownlie covered a mannequin in a side skating position with different suits built with panels with different types of roughness and proved that these types of suits were clearly able to improve the athlete’s performances.

Currently, most of the suits developed are optimized for relatively high speed sports (speed skating, cycling, etc.) and little focus was put on the optimization of low drag suits for low speed sport, such as running disciplines. In the previous work by the writing author [3] the focus was put on a preliminary garment optimization for 100m sprinting race, where the speeds are relative low (<15m/s). In this study the garment optimization was not focusing on the fabric itself, but the interaction between different topographies and the fabric structure. The main goal was to find out how the different scales (macroscales and microscales) present in the surface structure can influence the flow around a cylindrical body.

The representation of the overall surface as a combination of different topographic scales was

based on a simplified version of what is presented in Wieland *et al.*[15]. In this work a wavelength-dependent (“window”) roughness method is developed and different surface topographies with various roughness are seen a combination of macro, meso and micro scales. On top of these scales there is the hairiness. The simplified version used in [3] and in the present work consists in using only macroscale, microsocale and hairiness. The microstructure represents the fabric structure induced by the knitting or wrapping process. The macrostructure can be applied under the fabric to represent the overall modification of the fabric. The type of yarn used mostly gives the hairiness. **Figure 2** shows a coarse representation of these structures.

The hairiness was recently investigated by Bardal[16]. He concluded in his work that the hairiness present on most of the textiles due to the type of yarn used (mostly spun) has effect of eliminating the transition process and increasing the average drag in a similar matter to what happens on tennis balls[17].

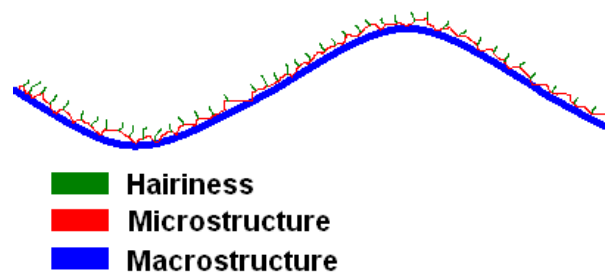


**Figure 2 - Definition of macro and micro roughness**

There are no currently deep investigations on how the different types of roughness interacts which each other. However in the previous project thesis[3] the different topographies (micro-macro scale) showed to have remarkable influence on how each type of roughness can influence the flow transition. Three different fabrics with different surface roughness and air permeability were used and placed over different number of strips representing the macrostructure of the fabric. All the fabrics used had no hairiness. Tests where the aerodynamic drag was measured were conducted in a wind tunnel using a cylindrical model. The results showed that the macrostructure can cause

remarkable changes in the total roughness and influence the flow transition at low critical Reynolds number with a consequent drop in drag coefficient,  $C_D$ . The results also showed that the different fabrics contribute in different ways. The rough fabric showed to have the ability to trigger the transition on the cylinder to lower critical Reynolds number than the smooth fabric, however combining a smooth fabric with the right number of strips it was possible to achieve very low critical Reynolds number and thus a large reduction in the drag coefficient,  $C_D$  at low speeds with the advantage of keeping a low  $C_D$  also at high speeds. A surface with no hairiness, low microroughness and high macroroughness was then found to be the optimal surface for disciplines like running, where the speeds are relative low (<10m/s) like.

The present work aims to further analyse the effect of the interaction of macro and micro roughness giving some basic guidelines for garment optimization in low speed sports. Two fabrics (one with smooth surface structure and one with rough surface structure) will be combined with different under layer and their performances on oval and tapered cylinders will be evaluated through wind tunnel testing. A full size suit made following these indications will then be designed and compared with the state of the art models from Adidas.

How the strips geometry influences the performance will be evaluated using strips with different thickness and width strips.

## II. STATE OF THE ART

The human body can be considered as series of bluff bodies with different dimensions, proportions, angles and inclinations. Horner[18] first postulated that the human body can be approximated as a series of circular cylinders and this approximation was also used by with success by Brownlie[19, 20] who carried out tests on circular cylinders to estimate the influence of textiles on the total drag of the athlete. Earlier studies by Oggiano[21, 22] and Chowdhury[23] used also the simplification in order

to selectively investigate different parameters that might play a role in the drag crisis phenomena: different types of surface roughness, air permeability, fabric stretching and fitting, seam positioning, etc. A recent study by Sæter [3] investigated the influence of flow transition by covering a cylinder with different fabrics and different under layer topographies.

Currently, infinite circular cylinders are the most common used model in wind tunnel experiments for drag optimization of sports garment. Flow around cylinders have also archived the most attention and was investigated by several authors and presented in details by Zdravkovich [4, 9].

A less crude approximation consists in considering the human body as series of finite oval and tapered cylinders with varying yaw angle ( $\lambda$ ) and angle of attack ( $\alpha$ ). During the running action, the body limbs constantly move and the air flow almost never hits the athlete body parts perpendicularly. The effect of different inclinations of the limbs due to the motions during a sprinting race is then crucial. The present work will investigate how different surface configurations (underlayer strips placed under different fabrics) will behave when it is placed over two different models: a finite oval cylinder and a finite tapered circular cylinder. Tests on the oval cylinder will be carried out at different angle of attack ( $\alpha$ ),  $0^\circ$ ,  $45^\circ$  and  $90^\circ$  and a yaw angle of  $45^\circ$ .

**Yaw angle:** During a sprinting race the athlete's bodies are in constantly different positions due to the motion of the athlete. The wind on the different body parts is therefore almost never coming from a normal direction (perpendicular to the athlete). Each body part will experience a different yaw angle ( $\lambda$ ) and a nice graphical representation was given by Grieve[24] and it is presented in **Figure 3**. He addressed the different angle, where thigh angle: the angle between the line of the thigh and the vertical. Knee angle: the angle between the extended line of the thigh and the line of the lower leg.

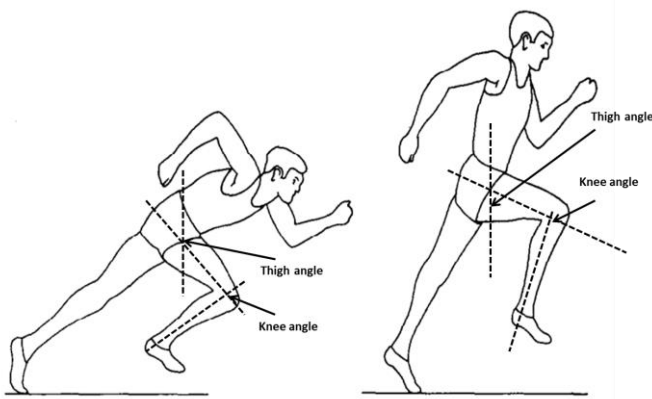


**Figure 3- Sprinter in a running posture, Angle-angle graph**

Oggiano[25] investigated four different yaw angles from  $0^\circ$ - $45^\circ$  on a finite cylinder covered with different textiles with various roughness levels. The results showed that with an increase of yaw angle  $0^\circ$ - $45^\circ$ , the critical speed and the consequent drag reduction gets smaller for all the roughness levels. However he noticed that the different roughness levels have different impacts on the  $C_{D\text{MIN}}$  relative to the different yaw angles.

**Finite bodies:** Previous experiments[26, 27] showed that the values for drag coefficient  $C_D$  for a finite length cylinder are lower than the values predicted from existing data for an infinite cylinder. With an increase in aspect ratio; the drag coefficient starts to increase and tends to infinity as  $L/D \rightarrow \infty$ . This is due to the frontal area, which appears in the dominator in the definition of  $C_D$ , approaching zero.

**Oval cylinders:** most of the previous tests on aerodynamics of sport garments used circular cylinders to represent the human body. However, some body parts (like the trunk) are more resembling to an oval cylinder than to a circular cylinder. The flowfield around a circular cylinder is different from the flowfield around an oval cylinder. This is mostly due to the fact that oval cylinders are not axisymmetric while circular cylinders are. They have a major and minor axis and they can have different orientations, relative to the direction of the flow. The orientation is defined with the angle of attack ( $\alpha$ ) **Figure 4**. Horner[18] pointed out that the pressure distribution around an oval cylinder is strongly dependent on the angle of attack ( $\alpha$ ). The pressure distribution is higher when the major

diameter is perpendicular to the flow direction and this to an increase in the drag coefficient,  $C_D$ . On the other hand, when the minor diameter is perpendicular to the flow, the  $C_D$  value is lower due to the boundary layer staying attached to the surface longer and the resulting pressure recovery.

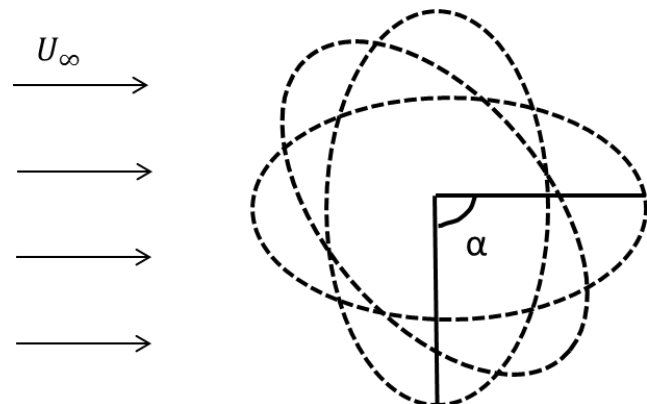


**Figure 4 - Oval cylinder, angle of attack ( $\alpha$ )  $0^\circ$ ,  $45^\circ$  and  $90^\circ$**

**Tapered cylinders:** The flow around a tapered cylinder is characterized by three-dimensional effects induced by linearly change in diameter. The influencing parameters are based on the taper ratio, defined as  $R_T = (d_2 - d_1)/l$ , where  $d_2$  and  $d_1$  being the major and minor diameter and the characterized length,  $l$ . Bosch[28] conducted wind tunnel experiments on tapered cylinders and compared with uniform cylinders. He and found out that the linearly change in diameter reduce the critical Reynolds number and the consequent reduction in  $C_D$ .

**Full Body vs. cylinders approximation:** Drag optimization in sports garment is often carried out using simplifications that the different body parts of an athlete is considered as different bluff bodies, to represent for example legs and arms. The limitations in using cylinders for aerodynamics tests of sports garment were shown in previous studies[19, 29]. D`Auteuil[30] used a 1:1 scale mannequin in a side push skating position to measure the drag and the surface pressure distribution. She found out that the flow developing around circular cylinders does not simulate properly the 3D flow around and the interactions of the flow around the multiple limbs of the body. The 3D flow

effects and limb interaction affected the local limb flow transition and the  $Re_{crit}$  of the limbs.

**Body parts accelerations and hysteresis:** During a sprinting race the athletes seldom assume a static posture and the speed of the limbs are constantly varying. While the upper body experiences a constant increasing speed, the upper and lower limbs experience positive and negative accelerations that differ from the average speed of the sprinter. This behavior is especially pronounced in sports where the legs are used in the propulsive phase (speed skating, running, cycling, etc.). A previous study [30] was able to capture and have a clear idea of the sprinters motion during a running phase. This study was carried out on sprinters using motion capture techniques which gave a clear understanding of how the different moving's parts (and particularly the legs) move during the running phase. A clear analysis of the stride cycle and the relative angles between trunk, thigh, calf and foot were monitored during the run of a sprinter and plotted versus each other. Combining these values with the average velocities during a 100 m race predicted in by Sykes in [31] it is possible to have a rough estimate of the local velocities on the different limbs. Currently, most of the research regarding sports garment aerodynamic relies on static drag force measurements for different increasing wind speeds and this might often lead to imprecise results since the effect of the local acceleration on the limbs is neglected. In static measurements, models are in fact tested with a constant and stable incoming flow, which is not simulating approximately the same as real conditions. Dynamic drag measurements carried out with the speed varying over time are therefore of practical importance in terms of garment optimization and also plays a relevant role in the overall drag reduction process.

The previous work carried out by the writing author [3] proved that the positive and negative accelerations that the body limbs experience during the run can lead to hysteresis cycles. This type of phenomena has previously been found and investigated on cylinders by a several authors [7, 8, 32]. They have all agreed that this type of hysteresis phenomena is related to the behaviour of the laminar boundary layer separation and transition.

The same behaviour as for cylinders have also been investigated and seen on stall and separation process in air foils, with the same explanation. The study has also concluded that the ability to the flow to remember its past history is responsible for the hysteresis phenomena. [33].

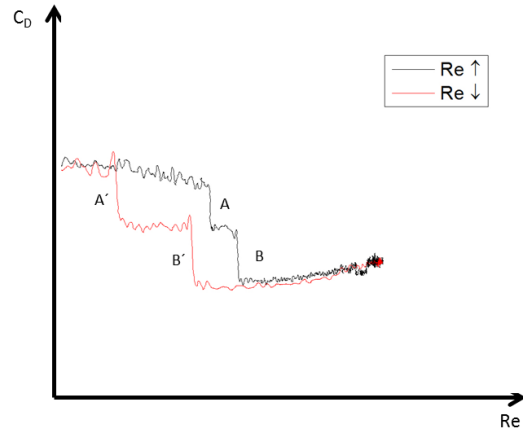


**Figure 5 - Hysteresis effects for transition A and B (increasing  $Re \uparrow$ ) and transition A' and B' (decreasing  $Re \downarrow$ )**

With respect to sports garment aerodynamic the hysteresis phenomena is of practical important because it results in to two different critical Reynolds numbers in the “drag crisis” process for increasing decreasing speed **Figure 5**. This behaviour was previously shown also by Schewe, which found that decreasing speeds leads to lower critical Reynolds number than increasing speed matching the findings shown in [3]. A particular attention to the drag crisis hysteresis process will also be given in the present work by measure lower accelerations than previous conducted by using a cylinder without the fabric configuration, to see the possible influence in the hysteresis phenomena.

### III. EXPERIMENTAL SETUP

#### A. Wind tunnel

In order to measure the aerodynamic drag acting on three different cylindrical geometries and a full scale mannequin, two different wind tunnels at the department of energy and process engineering at NTNU, Trondheim were utilised.

Drag measurements on the cylindrical models, oval, tapered and circular cylinders were performed in the small scale wind tunnel. The test section of the wind tunnel is 2.00 m long, 0.72 m high and 1.01 m wide. The wind tunnel is equipped with a 45 KW fan and the maximum reachable speed is ca. 40m/s.

Drag measurements on the real size mannequin were performed in the large scale wind tunnel as shown in **Figure 6**. The test section of the wind tunnel is 12.5 m long, 1.8 m high and 2.7 m wide. The wind tunnel is equipped with a 220 KW fan that can produce a variation speed between 0 – 30m/s.

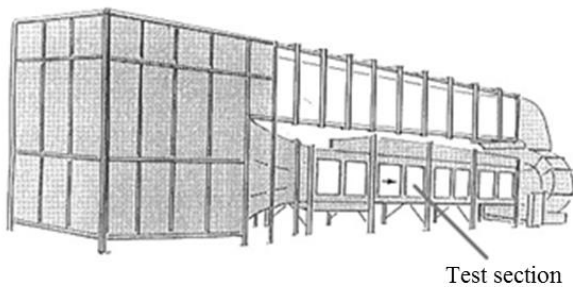


**Figure 6 - Large scale wind tunnel at the department of energy and process engineering at NTNU, Trondheim**

#### B. Drag measurement

The drag force component was measured by a six component force plate AMTI BP600400HF which has a natural frequency of 470 Hz. The force plate was used in both wind tunnels and positioned under the test section of the wind tunnel. A Pitot – static probe was used to measure the free-stream velocity and was placed in the flow with the axis parallel to the flow. The probe was connected to a pressure transducer and the acquired voltage output from the force plate and pressure transducer was logged by a LabView based logging program. The three different

cylindrical geometries and the real size mannequin was mounted in the wind tunnel and connected to the force plate by a steel support. All the drag measurements were conducted twice to ensure reliability.

### IV. METHODS

#### A. Dynamic and static measurement

Drag measurements were carried out using a hybrid technique which is a combination of static and dynamic measurements. This technique avoids the scattering which occurs in the dynamic measurements at low speeds ( $<7\text{m/s}$ ) due to high relative error in the computing of the drag coefficient.

The time varying dynamic measurements were conducted at ( $>7\text{m/s}$ ) by first increasing the wind tunnel speed to the maximum and successively decreasing the speed to zero. Time series were logged at a sampling frequency of 200 Hz and a sample time of 60 seconds. Low speeds ( $<7\text{m/s}$ ) from the dynamic measurements was removed in the results and replaced with static measurements which was conducted with different increasing wind speeds ( $<7\text{m/s}$ ). The static measurements were taken at a sampling frequency of 1000 Hz and a sample time of 40 seconds, which gives a total of 40 000 samples per measurements.

Measurements conducted in the small scale wind tunnel were taken with a speed range from 0 to 40m/s, which lead to different Reynolds range depending on the applied model. In the full scale wind tunnel it was only conducted static measurements with different increasing wind speeds ranging from 0-20m/s.

Because of the high frequency noise which occurs from the dynamic measurements it was needed to add filtering to extract the relevant data from the measurements. Data analysis software Origin pro8 has then been used as a tool for filtering the dynamic time series measurements. The filtering method used is a Fast Fourier transform (FFT) filtering based on Fourier transform which decomposes a signal from the time domain to frequency domain. High frequency noise was

removed with a low-pass FFT filter with a cut-off frequency of 10 Hz.

### B. Oval cylinder

The oval model used for the experiments is made of glass fiber and has a slender diameter of 11 cm, broad diameter of 16 cm and span length of 50cm. The oval cylinder was considered as finite length, where the free end of the top of the oval cylinder is exposed freely to the oncoming wind stream. The model was mounted in the small scale wind tunnel and connected to the force plate by two different steel supports arrangements, one in a vertical position where the model was placed perpendicular to the flow and the second steel support was design in a yaw angle ( $\lambda$ ) of 45 degrees inclined to the direction of the flow **Figure 7**.

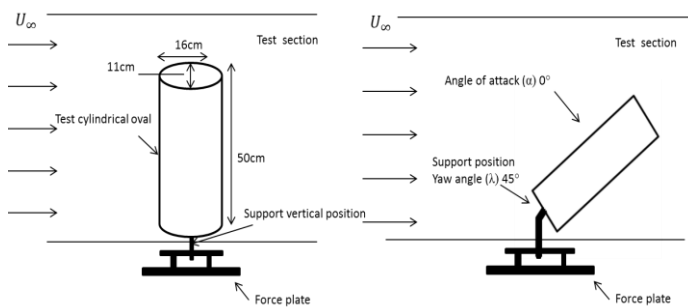


**Figure 7- Experimental setup, oval cylinder vertical and inclined position**

The experiments were divided into two parts, where the first test was conducted with a steel support in a vertical position and design in such way that the angle of attack ( $\alpha$ ) of the model can be adjusted, the oval cylinder model was then positioned with three different angles of attack  $0^\circ$ ,  $45^\circ$  and  $90^\circ$  degrees **Figure 8** **Figure 9** **Figure 10**, with the following frontal area of,  $0.08 \text{ m}^2$ ,  $0.0680 \text{ m}^2$  and  $0.055 \text{ m}^2$ . The aerodynamic forces were measured for a range of speeds of 0-20m/s and the Reynolds range varied dependent on the angle of attack used. The Reynolds number was based on the diameter used to calculate the frontal area (characteristic diameter in the flow direction), **Figure 8** **Figure 9** and **Figure 10**. The aspect ratio is defined as  $L/D$ , where  $L$  is the length of the oval cylinder and  $D$  is the diameter in the flow direction. The oval cylinder with angle of attack ( $\alpha$ ) of  $0^\circ$ ,  $45^\circ$  and  $90^\circ$  have the following aspect ratio 3.1, 3.7 and 4.5.

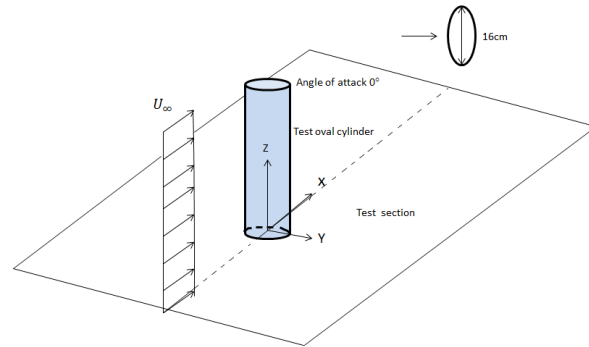


**Figure 8- Oval cylinder, angle of attack 0 degrees**

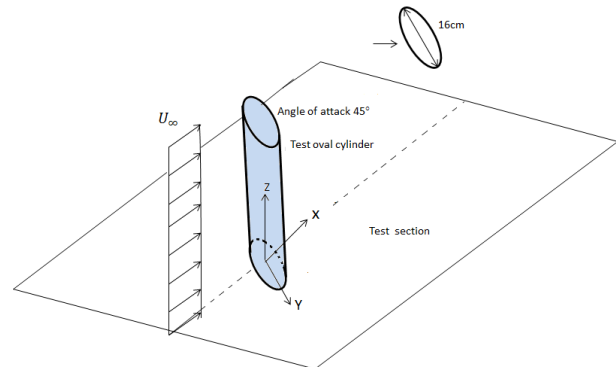


**Figure 9 –Oval cylinder, angle of attack 45 degrees**

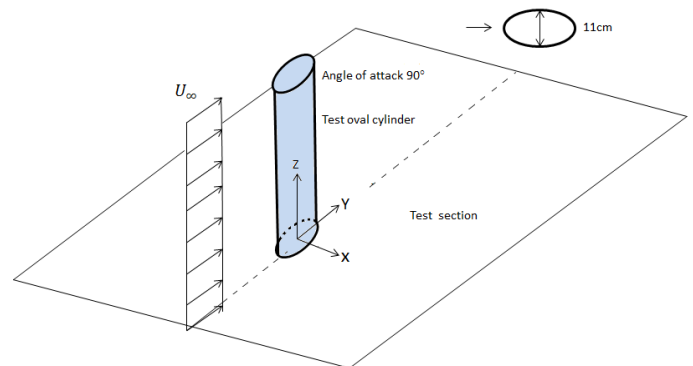


**Figure 10- Oval cylinder, angle of attack 90 degrees**

To evaluate the impact on the aerodynamic drag when the athlete position is non-vertical, the steel support arrangement was design to allow the oval cylinder to be fixed in a yaw angle ( $\lambda$ ) of 45 degrees and the oval cylinder was positioned with an angle of attack ( $\alpha$ ) of 0 degrees relative to the wind direction with the following frontal area of  $0.0663 \text{ m}^2$ . The model of inclined oval experimental arrangement is shown in **Figure 7**.

The aerodynamic forces were measured for a range of speeds of 0-20m/s and Reynolds number was based on the major diameter (0 degrees).

Drag data from the measurements of the oval cylinder positioned in both yaw and vertically position with an angle of attack ( $\alpha$ )  $0^\circ$  and the vertical oval cylinder positioned with an angle of attack  $45^\circ$  were corrected considering the wind tunnel blockage. The blockage effect is defined as the model frontal area to the cross-sectional area of the test section. The blockage effect was calculated to be 11 percent (yaw and vertical  $\alpha=0^\circ$ ) and 9.4 percent (vertical  $\alpha=45^\circ$ ) for the largest diameter. The value should be less than 7.5 percent[2] and was corrected in the calculation of drag. The formula[34] was used for the calculation:

$$\frac{F_C}{F_M} = 1 - k \frac{S}{A}$$

where  $F_C$  is the corrected value,  $F_M$  is the measured value,  $k$  is a constant of 2.84,  $S$  model frontal area and  $A$  is cross-sectional area.

During the experiments the oval cylinder for both angular positions was covered with 3 mm wide 2 mm thick rubber strips and placed under two different fabrics and measurements were conducted for both static and dynamic.

### C. Tapered cylinder

The tapered cylinder used for the experiments is made of glass fiber and has a minor diameter,  $d_1$  of 11 cm, major diameter,  $d_2$  of 16 cm, and span length of 50 cm, with a consequently frontal area of  $0.0675\text{m}^2$  **Figure 11**. The Reynolds number is based on the mean diameter is 13.5 cm.

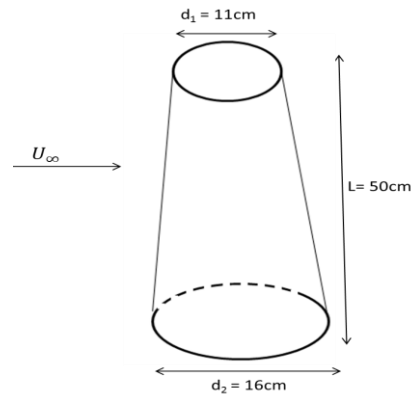


**Figure 11- Experimental setup tapered cylinder**

The tapered cylinder was mounted in the small wind tunnel and connected to the force plate with a steel support. During the experiments the tapered cylinder was also covered with the same strips and fabrics, used on the oval cylinder and the same measurement technique was used.

### D. Different accelerations

To evaluate how different accelerations affect the drag crisis, a cylindrical model made of PVC was used and placed in the small scale wind tunnel. The cylinder has a diameter of 16cm and length of 50cm and a smooth surface. The dimension was chosen to ensure that the critical Reynolds number could be reached. The blockage effect was neglected in this case.

Dynamic drag measurements were conducted. Time series were logged at a sampling frequency of 200 Hz. The measurements were conducted for a speed range 0-40m/s with six different accelerations **Figure 12**. The different accelerations are denoted in the results as A1, A2, A3, A4, A5 and A6, where A1 ( $1.33\text{ m/s}^2$ ) represents the time series with the highest acceleration and A6 ( $0.08\text{m/s}^2$ ) the lowest acceleration. The highest acceleration, A1 was used in all other dynamic measurements.

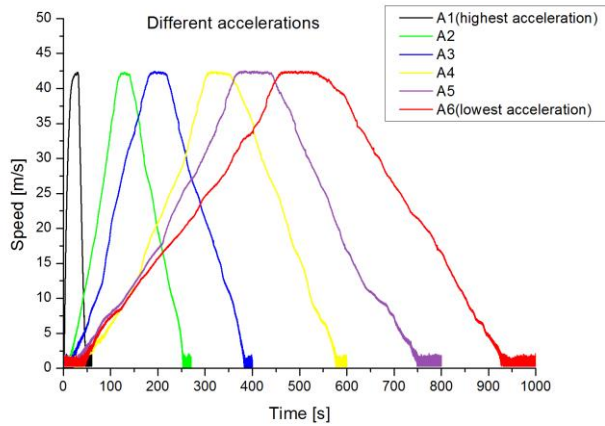


**Figure 12- Different accelerations**

### E. Surface structure

Two different fabrics with different roughness level and air permeability were used in the present work. The fabrics were placed on the oval and tapered cylinder models. The fabrics are the same fabrics used in the previous project thesis[3] and the same names were kept to be consistent. The fabrics are characterized by a different surface structure and they previously showed clearly different behaviours. The smoother fabric showed improved aerodynamic performances when a macro roughness (strips) was placed under it.

The first fabric denoted as T1 has a dimpled structure, and it is a stretchable fabric. The yarn type is filament and the fabric has high air permeability. The second fabric denoted as T3 is not a knitted textile but a plastic polyurethane based fabric with a very smooth surface texture, low stretching properties and it is impermeable **Table 1**. The fabrics were fitted to the models in the same way with a stretching coefficient of 23%.

**Table 1- Properties for each textile**

Fabric (Structure type)	T1	T3
<i>Yarn type</i>	Filament	-
<i>Surface structure</i>	Dimpled	Smooth
<i>Permeability</i>	Permeable	Impermeable

### F. Under layer strips

During the experiments the oval and tapered cylinders were covered with 3 mm wide and 2 mm thick rubber strips. The strips were attached to the surface of the different geometries in the axial direction and placed under fabric T1 and T3 in order to represent the modifying macrostructure of the fabric. The strips were placed with an equal distance,  $L$  between the adjacent strips and fabric samples were placed over, **Figure 13** paying attention to position and the seam on the downstream side of the models. The distance between the strips was systematically changed and half of the strips were removed between each round in order to double the distance between them. For the current experiment it was chosen to use 32, 16 and 8 strips. Measurements with only fabric placed on the models without the strips were conducted for comparison.

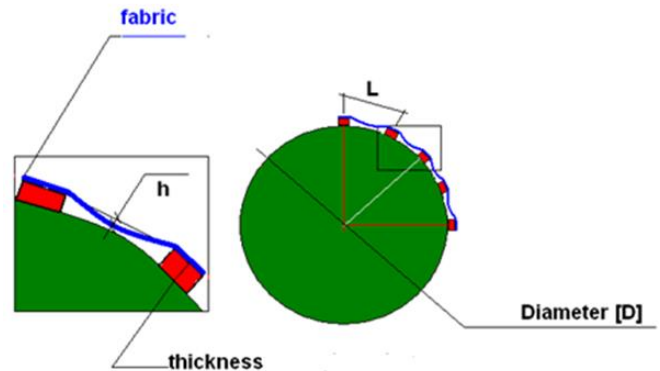


**Figure 13 - Concept for the strips attached to the model, with equal distance between the strips**

The oval and tapered cylinder were tested with the same number and size of the strips, but since they have different geometries and dimension the properties of the length between the strips varies as shown in **Table 2****Table 3**.

**Table 2 - Oval cylinder, number of strips and length between two strips**

Number of strips	Thickness and width of the strips [mm]	Length between two strips (center to center) [mm]
32	2×3	10.44
16	2×3	23.87
8	2×3	50.75

**Table 3- Tapered cylinder, number of strips and length between two strips**

Number of strips	Thickness and width of the strips [mm]	Length between two strips (center to center) [mm]	
		$d_1=11\text{cm}$	$d_2=16\text{cm}$
32	2×3	10.80	15.70
16	2×3	21.60	31.41
8	2×3	43.20	62.83

Strips size: To investigate how the strips size influences the  $C_D$ -Re curves, additional drag measurements with strips characterized by different thickness and width were conducted. In this specific case, a cylindrical model made of PVC was used for the experiments. The model is the same used in [3]. The circular cylinder used has a diameter of 11 cm, length of 40 cm and a consequently frontal area of  $440\text{ cm}^2$ . The experiments were performed in the small scale wind tunnel with the same setup as for the other tests. The cylindrical model was covered with four different strips samples provided by Adidas **Table 4** Each sample has the same number of strips, but the strip size is different. The strips samples are denoted as 1a to 1d.

**Table 4- Different thickness and width of the strips**

Strips sample	Number of strips	Thickness and width of the strips [mm]	Length between two strips (center to center) [mm]
1a	24	1×1	1.2
1b	24	1×3	1.0
1c	24	3×1	1.2
1d	24	3×2	1.0

Strips sample 1d are shown in **Figure 14**, where strips made of rubber are attached on the outside surface of the fabric. Each strips sample was placed under fabric T1 and T3 in order to represent the macrostructure of the fabric. Additional tests without fabrics placed on the strips were carried out.

**Figure 14 - Strips sample 1d (3×2mm)**

### G. Suits

In order to establish how different suits can affect the total drag actin on a human body, a real size mannequin of an athlete in a static running posture was used. The tests were carried out in the full scale wind tunnel. The mannequin tested is made of glass fiber, with a height of 1785.61 mm and a frontal area  $0.4774\text{ m}^2$  **Figure 15**.



**Figure 15 - Mannequin, running posture with height of 1785.61 mm**

The mannequin was mounted in the wind tunnel and drag measurements were conducted with the same force plate used in the small scale wind tunnel (AMTI BP600400HF). The experimental setup is shown in **Figure 16**. The force plate was positioned under the test section of the wind tunnel and the mannequin was connected to the force plate with a steel support fixed in the back of the mannequin **Figure 16**. During the experiments the mannequin was dressed with three suits made by Adidas and one suit developed at NTNU in order to evaluate the effect of each suit. Drag measurements were conducted in a range of speed from 0-20m/s, as static measurements and a  $C_D$ -Speed curve has then been plotted. The static measurements were taken at a sampling frequency of 1000 Hz and at a sampling time of 40 seconds, which gives a total of 40 000 samples per measurements. All drag measurements were conducted twice, to ensure reliability.

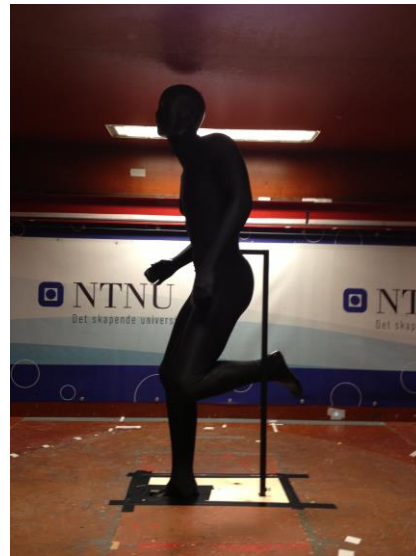


**Figure 16 - Experimental setup mannequin**

### ***Adidas suits:***

The suits developed by Adidas were made based on the preliminary results from the previous project thesis [3]. All the suits were fitted to the mannequin in the same way with equal stretching. The fabric structure was the same for all suits tested a smooth/filament, permeable and stretchable. The suits developed by Adidas were denoted as A1, A2 and A3, shown in **Figure 17** **Figure 19** and **Figure 20**.

### ***Suit A1:***

The suit A1 (**Figure 17**) is covered with a combination of strips (different thickness and width) and dots made of rubber placed on the outside surface of the fabric. The backside surface was without this configuration.



Figure 17 - Mannequin low drag suit A1, with strips placed on the outside

Figure 18 shows in detail how the strips and dots are assigned to each part of the suit.



Figure 18 - Low drag suit A1, detailed

### *Suit A2:*

The suit A2 (Figure 19) is the same suit as A1 (Figure 17), but turned on the inside out, so that the configuration of the strips and dots are on the inside surface. The strips and dots will then work as a under layer and allow the fabric to form a macrostructure which has shown in the previous finding[3] to be beneficial because it is possible to achieve low critical Reynolds number with a consequent drop in the drag coefficient,  $C_D$ .



Figure 19 - Mannequin low drag suit A2, with strips placed on the inside

For comparison, a plain suit without strips and dots was tested, A3 (Figure 20). The fabric used for this suit is the same used in A1 (Figure 17), but with no interventions.



Figure 20 - Mannequin low drag suit A3, without strips

### *NTNU suit:*

The suit is a combination of the suit A3 (Figure 20) with a modified under layer. The under layer was developed assuming (from previous experiments) the right combination of strips and fabric that allows to shift the transition from laminar to turbulent regime (in cylinders, oval and tapered) at the needed speed.

The under layer strips were placed treating each body part as a particular geometrical shape with

varied dimension and position (angle of attack and yaw angle) **Figure 21**. The upper part of the body and the calf were considered as tapered cylinders, while the arms and the legs were considered as circular cylinders and oval cylinders with different dimension and position.

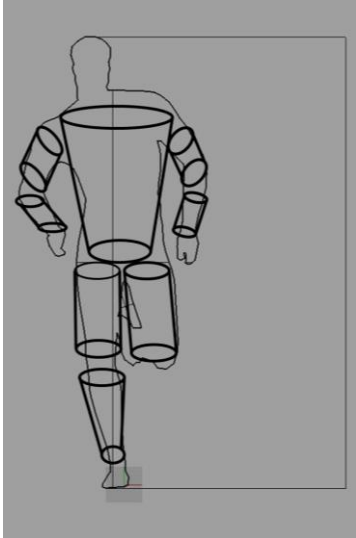


**Figure 21-** Concept drawing of the mannequin, with different geometrical shapes

The manipulated under layer was custom made placing rubber strips directly on the mannequin. The strips had different thickness and width and were attached to the mannequin surface in the axial direction and placed under the suit A3. The strips were placed with an equal distance,  $L$  from the adjacent strip on both limbs and arms, but the length between two strips was varied relative to the different body parts, due to the dimensions of each body parts differs from each other. The upper arm and lower arm were covered with a strips distance between two strips respectively of 5cm and 3cm. The upper and lower limbs were covered with strips placed with a distance of 6cm and 3cm between them. Both front and back side of the mannequin legs **Figure 22** and arms **Figure 23** were covered with strips to ensure symmetry. Strips were only placed on the sides of the trunk **Figure 23**, with the knowledge that the interface between the front and backside of the mannequin is the area where the flow separates and thus a beneficial place to cover strips in terms of drag reduction.



**Figure 22 -** Mannequin legs covered with strips



**Figure 23 -** Mannequin arms covered with strips

## V. RESULTS AND DISCUSSION

### A. Oval cylinder, angle of attack ( $\alpha$ )

In this section the results relative to the oval cylinder vertically placed in the wind tunnel is presented and discussed. Tests were carried out with three different angles of attack ( $\alpha$ ),  $0^\circ$  (major diameter in the flow direction),  $45^\circ$  and  $90^\circ$  (minor diameter in the flow direction). **Figure 24** to **Figure 29** show the non-dimensional drag coefficient,  $C_D$  plotted versus the Reynolds number for each angle of attack. The plots show the results for T1 and T3 with and without strips placed in the underlayer. The results presented are based on the hybrid technique where the low Reynolds number ( $<7 \times 10^4$ ) from the dynamic measurements are

replaced with static measurements. The aerodynamic drag was measured for a speed range from 0 to 40m/s which lead to different Reynolds range based on the applied model.

Comparing the results for the configuration with the strips placed under fabrics T1 and T3 with the results for the same fabrics without strips, some clear differences can be seen for all the angles of attack ( $\alpha$ ), (Figure 24-Figure 29). The airflow around the model covered with only fabric (without strips) remains laminar at higher Reynolds number before it reaches the drag crisis. However, when the strips are placed under the fabric, the boundary reaches transition at much lower speeds. Similar findings were found in the previous results tested on a cylindrical cylinder[3] where the under layer strips showed to trigger the flow transition at lower wind speed. These results confirms that, regardless the shapes of the models applied and the different angles of attack ( $\alpha$ ) it is possible to trigger early transition at low critical Reynolds numbers with a consequent drop in  $C_{D\text{MIN}}$  by introducing a modified under layer.

The results show clearly that the  $C_D$  values are largely dependent on angular position ( $\alpha$ ) and they are presented in Figure 24 and Figure 29. The plots clearly show that larger angles of attack generate lower  $C_D$  confirming the theory[18]. However this type of behavior was not found for all the surface configurations. Some surface configurations show the opposite effect where the increase of angle of attack ( $\alpha$ ) decreases the  $C_D$  values.

Figure 24 and Figure 25 show are relative to the oval cylinder with an angle of attack ( $\alpha$ ) of  $90^\circ$  (minor diameter in the flow direction). The oval cylinder in this case has a streamlined shape which leads to a lower  $C_D$ . Both fabrics, T1 and T3 achieve good results with the under layer strips placed under the fabrics resulting in large reduction of  $C_{D\text{MIN}}$  at low Reynolds numbers. The  $C_D$  values in the supercritical regime are also lower than the ones found in the configuration with no under layer. However, with respect to garment optimization and running disciplines where the speeds are relative low (<15 m/s), 16 strips used as macrostructure for fabric T1 and T3 showed to have the best outcome. The results show also relative low  $C_D$  values, which

have shown in the literature[26, 27] to be common for short finite cylinders with high aspect ratio. The aspect ratio for the oval cylinder,  $90^\circ$  is 4.5.

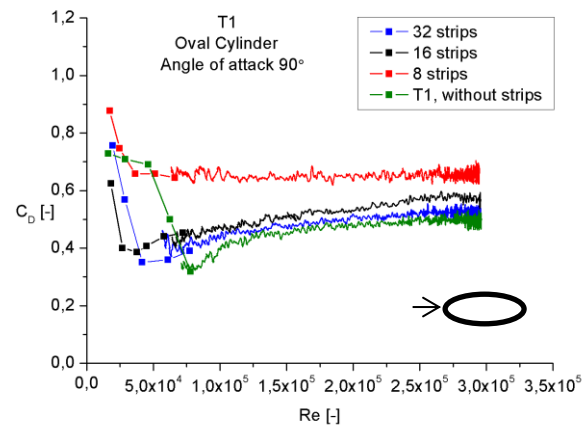


Figure 24 –  $C_D$  - Re curve for oval cylinder, angle of attack  $90^\circ$ , textile T1

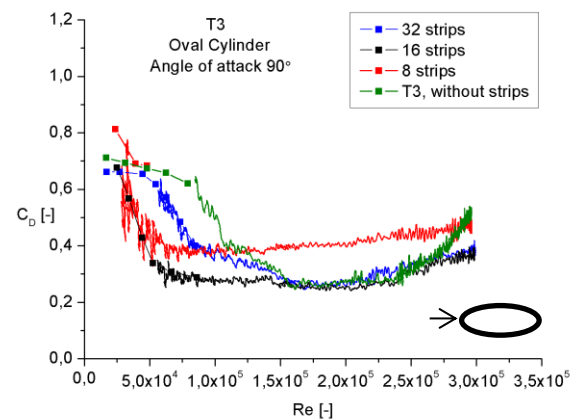


Figure 25 –  $C_D$  - Re curve for oval cylinder, angle of attack  $90^\circ$ , textile T3

Figure 26 and Figure 27 are relative to the oval cylinder positioned with an angle of attack ( $\alpha$ ) of  $0^\circ$  (major diameter in the flow direction). This results in a very low aspect ratio of 3.1. The results show that when the angle of attack ( $\alpha$ ) increases, the transition from laminar to turbulent it not so apparent, excluded without strips (fabric T1), and 32 strips placed under fabric T1. Both surface configurations showed in the results to have the ability to shift the transition from laminar to turbulent. The results also show that the  $C_D$  values are almost constant in the supercritical regime for both fabrics, T1 and T3. The  $C_D$  values can be observed to be relative low. The reduction in  $C_D$  have shown in previous experiments [26, 27] to be

in agreement with the literature for finite model with high aspect ratio.

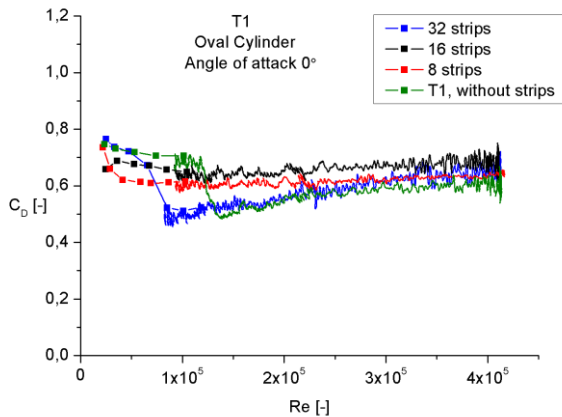


Figure 26 –  $C_D$  - Re curve for oval cylinder, angle of attack  $0^\circ$ , textile T1

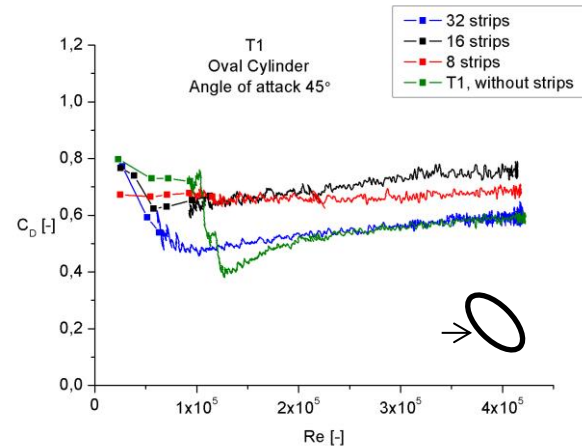


Figure 28 –  $C_D$  - Re curve for oval cylinder, angle of attack  $45^\circ$ , textile T1

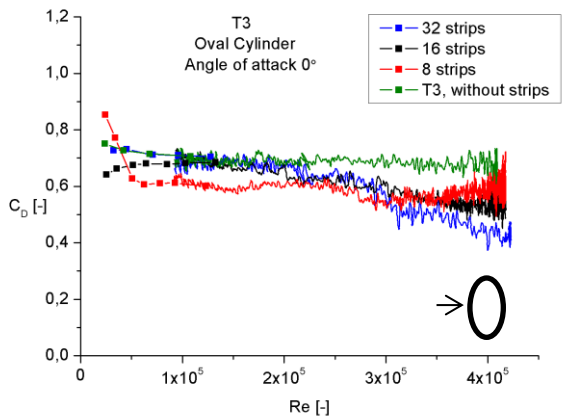


Figure 27 –  $C_D$  - Re curve for oval cylinder, angle of attack  $0^\circ$ , textile T3

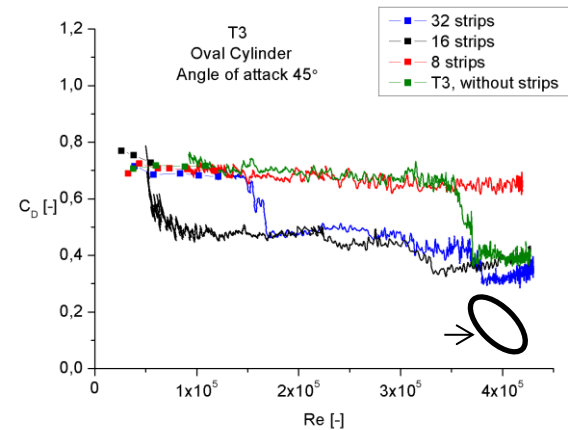


Figure 29 –  $C_D$  - Re curve for oval cylinder, angle of attack  $45^\circ$ , textile T3

The results plotted **Figure 28** and **Figure 29** show the oval cylinder positioned vertically with an angle of attack of  $45^\circ$ , aspect ratio 3.7. The results show that there are different effects wherever the fabric has a rough surface structure, T1 or a smooth surface structure, T3. Fabric, T1 **Figure 28** is able to shift transition to lower critical Reynolds numbers than for fabric, T3 **Figure 29** (32 strips and without the strips). The results also show that 16 strips placed under the two different fabrics remarkably affect the flow transition lowering the critical Re. With a smooth surface structure it is possible to maintain lower critical Reynolds numbers with a consequent drop in  $C_{D\text{MIN}}$  than for rough fabric, T1. Regarding sports garment aerodynamic 16 strips placed under a smooth surface is most beneficial, because it is possible to achieve reduction in critical Reynolds number and thus a reduction in  $C_D$  values.

### B. Oval cylinder, yaw angle ( $\lambda = 45^\circ$ )

During a sprinting race the athlete's arms and legs is almost never perpendicular to the flow. The angle of the legs and arms varies constantly, it is therefore important to evaluate how the modified surface structure affects the flow when the yaw angle ( $\lambda$ ) changes. In this section the results from the oval cylinder fixed in a yaw angle ( $\lambda$ ) of  $45^\circ$  and positioned with an angle of attack ( $\alpha$ ) of  $0^\circ$  is presented and discussed. **Figure 30** and **Figure 31** shows the non-dimensional drag coefficient,  $C_D$  plotted as a function of Reynolds number ( $0-4.5 \times 10^5$ ) and the results shows how each fabric, T1 and T3 behave when adding strips under the fabrics. For comparison results regarding the fabric

mounted on the oval cylinder without strips are presented in the same figures.

The results for the rough fabric T1, **Figure 30** shows that the different numbers of strips (32, 16 and 8 strips) placed under the fabric, have almost the same impact on the drag coefficient,  $C_D$  values in the supercritical regime when the oval cylinder is inclined. The only differences are in the transition area ( $0-1.0 \times 10^5$ ) where the flow goes from laminar to turbulent. In this regime it is possible to observe that the different number of strips have influence on the critical Reynolds. The results show that fabric combined with all the different number of under layer strips have the ability to achieve lower critical Reynolds numbers then without the strips, where only the fabric is present.

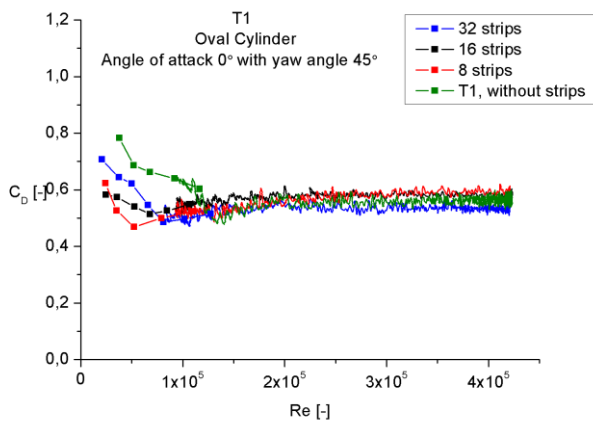


**Figure 30 –  $C_D$  - Re curve for oval cylinder, angle of attack  $0^\circ$  and yaw angle  $45^\circ$ , textile T1**

The results for the smooth fabric T3, **Figure 31** shows that the  $C_D$  values are almost constant over the entire flow field; however the results show clearly that the strips the model with strips reaches lower  $C_D$  values than the model without.

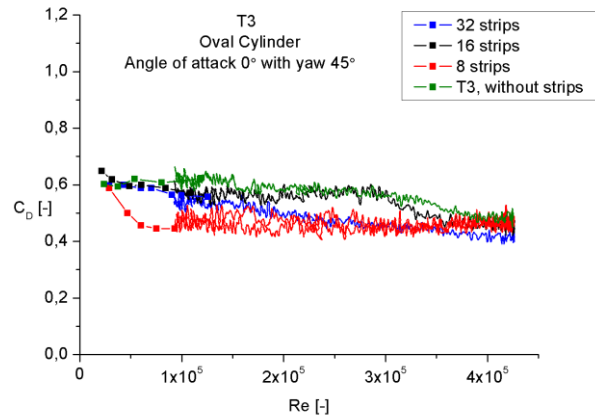


**Figure 31–  $C_D$  - Re curve for oval cylinder, angle of attack  $0^\circ$  and yaw angle  $45^\circ$ , textile T3**

By comparing the results presented in **Figure 30** **Figure 31** with the oval cylinder positioned vertically with an angle of attack ( $\alpha$ ) of  $0^\circ$  **Figure 26** **Figure 27**. The results show that with an increase in yaw angle from  $0^\circ$ - $45^\circ$  the drag coefficient,  $C_D$  values decreases. This confirms the findings presented by Oggiano[25] who noticed that for larger yaw angles, the drag reduction is smaller. The result in **Figure 30** and **Figure 31** shows also relative low  $C_D$  values. The reduction in  $C_D$  was found in previous experiments[26, 27] to be in agreement with the literature for finite model with high aspect ratio.

### C. Tapered cylinder

In this section the results from the tapered cylinder are presented and discussed. **Figure 32** and **Figure 33** show the drag coefficient,  $C_D$  plotted against Reynolds number. The results presented are based on the hybrid technique. The speed range is from 0-40 m/s which leads to a Reynolds range from 0 –  $3.5 \times 10^5$ .

The results shows clearly different effects whether the textile is smooth, T3 or rough, T1. The results for the rough fabric, T1 are shown in **Figure 32**. The results show that for a single fabric itself without strips it is possible to trigger transition to very low critical Reynolds numbers, however by introducing a modified under layer to a rough surface structure the results shows that it is possible to achieve lower critical Reynolds number than for the fabric without strips. The disadvantage is in the supercritical

regime after transition occurs where the  $C_D$  values starts to increase abruptly which results in increasing  $C_D$  values.

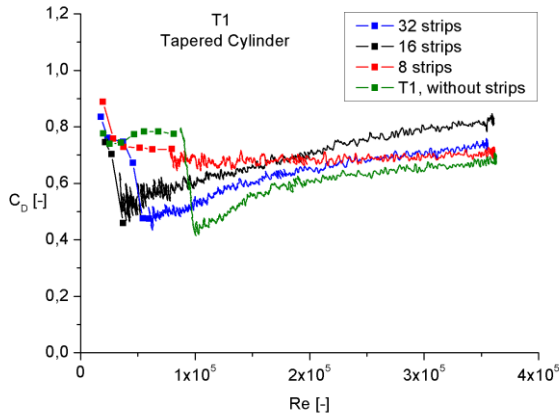


**Figure 32 –  $C_D$  - Re curve for tapered cylinder, textile T1**

A completely different behavior can be seen in **Figure 33** where the modified under layer is combined with a smooth fabric, T3. This combination creates a type of roughness where only macro structure is present. This type of roughness can shift transition to low critical Reynolds numbers (depending on the number of strips) with low  $C_{D_{MIN}}$  values. The additional advantage is that the  $C_D$  values remain low in the supercritical regime allowing a constant drag reduction in the whole range. In the transitional regime where the flow goes from laminar to turbulent it can be observed for fabric T3 without strips and fabric T3 with 32 strips two unsymmetrical transition jumps which is called in the literature single and two bubble regime. This behavior results in different critical Reynolds numbers. The two unsymmetrical transition jumps are confirmed theory and separately described by Schewe[8, 32, 35] and Zdravkovich[4, 9]

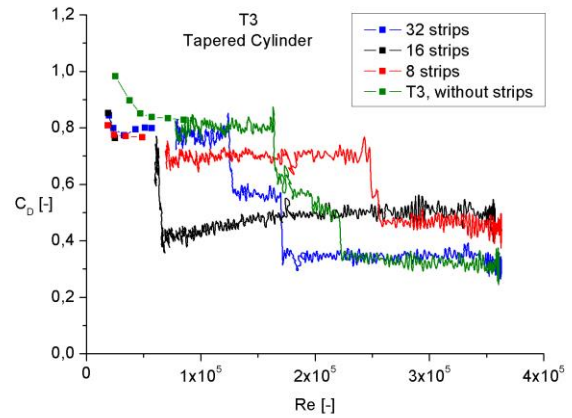


**Figure 33 –  $C_D$  - Re curve for tapered cylinder, textile T3**

The results showed to have almost exactly similar behavior if compared with the results relative to the circular cylinder presented in the previous project thesis[3]. The results presented in this study showed that by using the right number of strips (16 strips) placed under fabric, T3 it is possible to trigger early transition resulting in both reduction in critical Reynolds number and a consequent drop in  $C_{D_{MIN}}$  value. By using rough surface structure it was possible to achieve very low critical Reynolds numbers, but the  $C_{D_{MIN}}$  values was higher than for smooth fabric, T3. This indicates that circular cylinder and irregular cylinder experience similar types of behavior over the entire flow field. However the results from the tapered showed lower critical Reynolds numbers than for the cylinder in the previous work. This confirms with the findings by Bosch[28].

#### *D. Size properties of the strips and fabric structure*

All the results in the previous report were relative to a circular cylinder [3]. The same model was used in the present work to investigate how thickness and width of the strips affect the flow field and the drag crisis process. Four different strips samples (1a-1d), with the same number of strips (24), were used in this test. The strips had different thickness and width and they were placed under fabric T1 and T3. **Figure 34** and **Figure 35** show the drag coefficient,  $C_D$  plotted against Reynolds number, Re for each fabric (T1 and T3) placed over the different strips samples (1a-1d). The results are presented in a Reynolds range from  $0-3.0 \times 10^5$  (0-40 m/s). The results show

that there is no remarkable difference between the different thickness and width of the strips in terms of drag coefficient,  $C_D$ . A general trend is that a smaller thickness and width (1×1mm) is able to trigger earlier transition a lower critical Reynolds numbers for both fabrics, T1 and T3. The different strips structure showed to only have visible influence in the critical regime where the flow goes from laminar to turbulent for fabric, T3 **Figure 35**. Previous study [3] conducted with a smooth fabric structure placed over different numbers of strips have shown that smooth fabrics seems to be more sensitive in the drag crisis area than rough surface structure, which can be the reason why the different strips sample show variations in critical Reynolds numbers in the transitional area, which leads still to the assumption that smooth surface structure are more sensitive in the transitional area than rough fabrics. With respect to optimization of sports garments aerodynamics it is important to consider the size properties when the strips are placed under a smooth fabric.

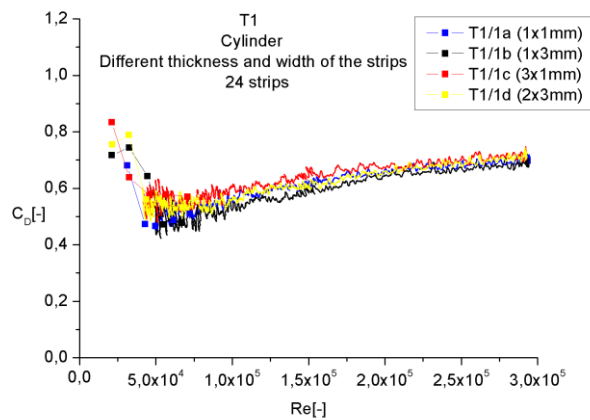


**Figure 34 –  $C_D$ -Re curve for cylinder, textile T1 placed over different strips samples with different thickness and width of the strips**

The two unsymmetrical transition jumps can be observed in **Figure 35**, where the drag coefficient,  $C_D$  first drops to ca. 0.6 and then at higher Reynolds number a new transition occurs with another consequent drop in drag coefficient,  $C_D$  ca. 0.4. The unsymmetrical transition jumps are confirmed in the theory[4, 8, 9, 32, 35] with the explanation that transition in the boundary layer occurs first on one side of the cylinder, “single bubble” and then at higher Reynolds on the other side of the cylinder, “two bubbles”.

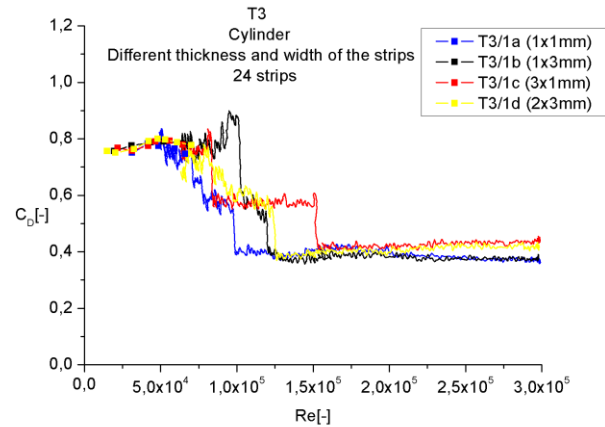


**Figure 35 –  $C_D$ -Re curve for cylinder, textile T3 placed over different strips samples with different thickness and width of the strips**

**Figure 36** shows the  $C_D$ -Re plots for the four strips samples (1a-1d) used in the previous section, but without the fabrics placed over. This means that the strips are placed directly on the fabric surface and directly interact with the boundary layer. The results show clearly that this type of configuration does not have the same advantage as when the strips are placed under the different fabrics, T1 and T3. With this type of configuration the fabric will experience a relative higher surface roughness, resulting in higher  $C_D$  values, which is not beneficial. The results indicate then the importance and the advantage by placing strips under the fabric to represent the macrostructure.

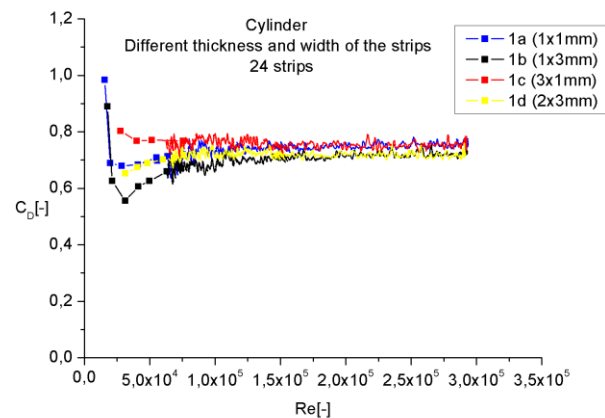


**Figure 36 –  $C_D$ -Re curve for cylinder with strips samples with different thickness and width of the strips, without fabric T1 and T3**

### E. Hysteresis

In this section will it be discussed the hysteresis phenomena which occurs in the dynamic measurements when increasing and decreasing the wind speed. The results presented in **Figure 37** and **Figure 38** are presented for both increasing Reynolds number,  $Re \uparrow$  and decreasing Reynolds number,  $Re \downarrow$  and plotted against the non-dimensional drag coefficient,  $C_D$ . The Reynolds range varies from  $4.5 \times 10^4$  to  $3.5 \times 10^5$  (0-40m/s). The results are not presented using the hybrid technique so the low Reynolds numbers ( $< 4.5 \times 10^4$ ) are removed because of the high relative error in the drag coefficient computation. Both figures represent the results conducted on the circular cylinder. **Figure 37** shows fabric T1 (rough surface structure) placed over under layer sample 1b (1mm $\times$ 3mm rubber strips) and, **Figure 38** shows fabric T3 (smooth surface structure) placed over under layer sample 1b (1mm $\times$ 3mm rubber strips). The two asymmetrical transition jumps (double bubble) and hysteresis cycle can clearly be observed in **Figure 38**. This behavior can often be seen in the transition area where the flow goes from laminar to turbulent. Schewe and Zdravkovich [4, 7, 8, 32] This study confirms that the hysteresis phenomena are related to the behavior of laminar boundary layer separation and transition on the cylinder. A similar behaviour can also be seen in the stall and separation process in airfoils where it is known that the hysteresis process is closely related to the behaviour of the laminar boundary layer separation and the ability of the flow to remember its past history is responsible for the hysteresis behaviour[33]. **Figure 38** shows also significant variations of critical Reynolds numbers for decreasing increasing speed which confirms with the findings by Schewe[35].

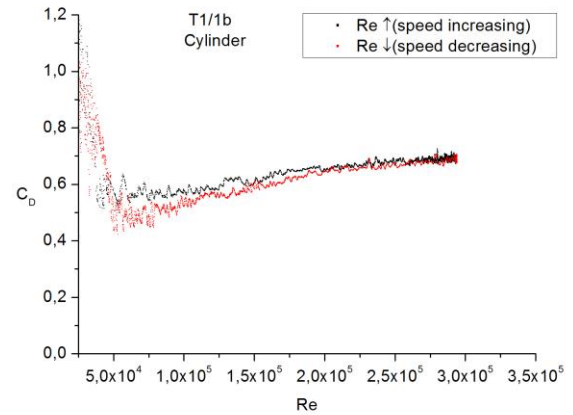


**Figure 37 –  $C_D$ - $Re$  curve, cylinder for dynamic measurements increasing,  $Re \uparrow$  and decreasing,  $Re \downarrow$ , fabric T1**

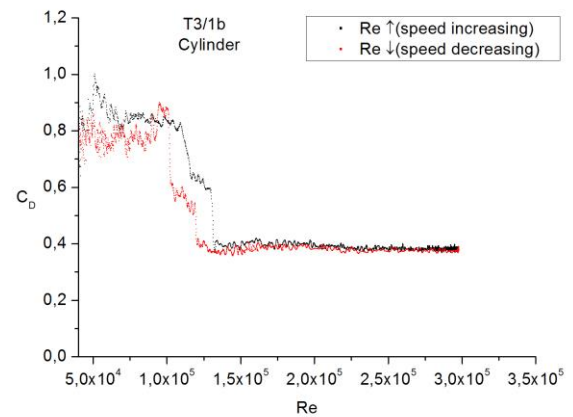


**Figure 38–  $C_D$ - $Re$  curve, cylinder for dynamic measurements increasing,  $Re \uparrow$  and decreasing,  $Re \downarrow$ , fabric T3**

The results in **Figure 37** and **Figure 38** shows that there are remarkable difference in the hysteresis cycle wherever the fabric has a rough surface structure, T1 or a smooth surface structure, T3. The hysteresis loop appears to be more pronounced for T3 than for T1, which are the same findings as in the previous results (same fabrics tested)[3]. This leads still to the assumption that smoother fabrics might be more sensitive to hysteresis than rough surface structure or that the hysteresis cycle was not able to be catch when the wind tunnel speeds are very low.

**Figure 39-Figure 43** for tapered and oval cylinder show  $Re_{crit}$  plotted against number of strips for both increasing,  $Re \uparrow$  and decreasing,  $Re \downarrow$  for each fabric, T1 and T3. All figures show that higher surface roughness, T1 is able to trigger early transition

resulting to lower critical Reynolds numbers than for smooth surface structure, T3. This occurs regardless of which model (oval and tapered) was used. The results from **Figure 39-Figure 41** show also that when the surface structure is smooth, T3 the hysteresis cycle appears to be more pronounced than for a fabric with high surface roughness, T1. Both findings were found in the previous work [3] carried out on a circular cylinder. The results in **Figure 42** and **Figure 43** show that the hysteresis phenomena do not occur when the oval cylinder is placed vertically with an angle of attack of  $0^\circ$  and with an inclined yaw angle of  $45^\circ$  positioned with an angle of attack  $0^\circ$ . The results also shows that the same critical Reynolds numbers can be achieve wherever the model are in a inclined position or in a vertically position, this is not the case for fabric T3 with 16 strips placed under. The results shows that it is possible to achieve lower critical Reynolds number for a vertically position than for an inclined position.

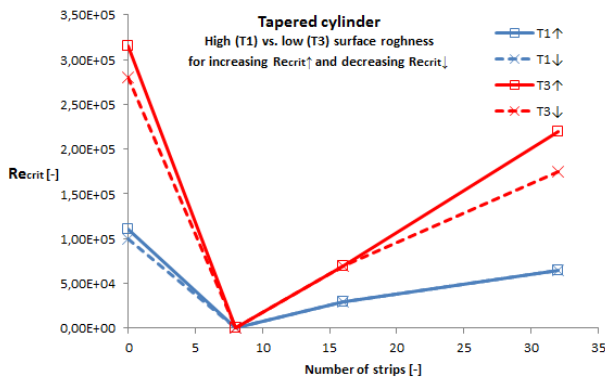


**Figure 39 - Tapered cylinder. Recrit vs. number of strips for both increasing,  $Re\uparrow$  and decreasing,  $Re\downarrow$  for each textile, T1 and T3**

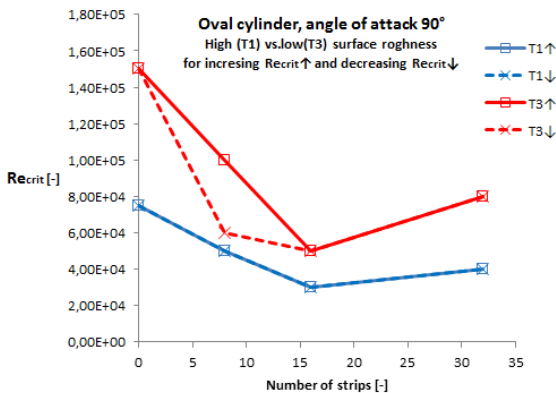


**Figure 40- Oval cylinder  $90^\circ$ , Recrit vs. number of strips for both increasing,  $Re\uparrow$  and decreasing,  $Re\downarrow$  for each textile, T1 and T3**

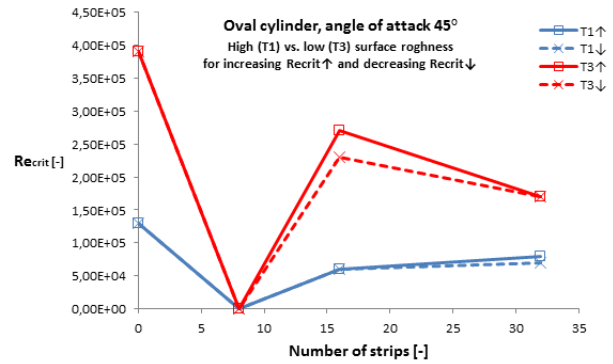


**Figure 41- Oval cylinder  $45^\circ$ , Recrit vs. number of strips for both increasing,  $Re\uparrow$  and decreasing,  $Re\downarrow$  for each textile, T1 and T3**

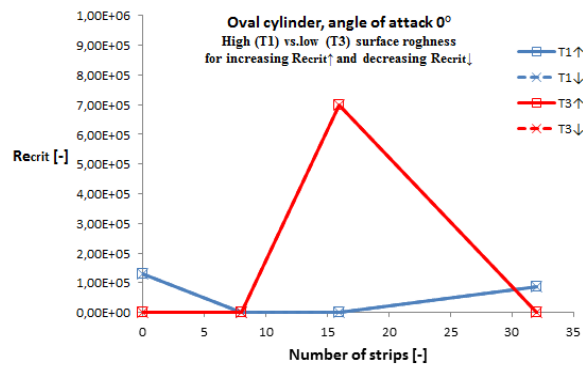


**Figure 42- Oval cylinder  $0^\circ$ , Recrit vs. number of strips for both increasing,  $Re\uparrow$  and decreasing,  $Re\downarrow$  for each textile, T1 and T3**

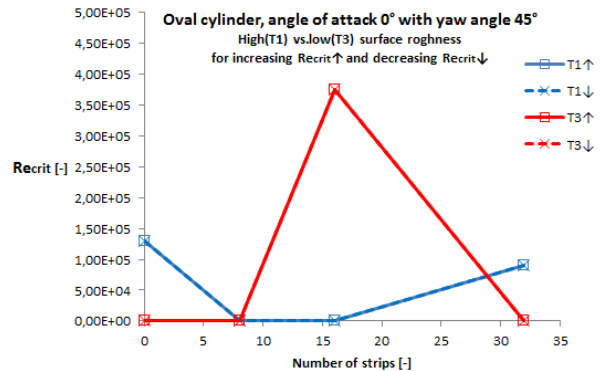


**Figure 43- Oval cylinder  $0^\circ$ , yaw angle  $45^\circ$ . Recrit vs. number of strips for both increasing,  $Re\uparrow$  and decreasing,  $Re\downarrow$  for each textile, T1 and T3**

## F. Different accelerations

In this section results relative to how the six different accelerations are able to affect the drag hysteresis phenomena are presented and explained. The drag force results from the dynamic time varying measurements was calculated and plotted against the speed **Figure 44**. The measurements were conducted on a smooth PVC cylinder without strips or fabric, using the same speed range from 0-40m/s but with six different accelerations **Figure 44**. The different acceleration are ranging from A1 to A6 were A1 ( $1.33 \text{ m/s}^2$ ) represents the time series which has the lowest sampling time (and thus the highest acceleration) and A6 ( $0.08\text{m/s}^2$ ) the highest sample time (and thus the lowest acceleration) **Figure 44**. The hysteresis loop can clearly be observed for a speed range lying between 29-38m/s. The hysteresis and the break in the symmetry with two discontinuous transitions (single and double bobble) can also clearly be observed **Figure 44** in the transition state where the flow goes from laminar to turbulent. confirming the findings of Schewe [7, 8, 35] and Zdravkovich[4, 9],

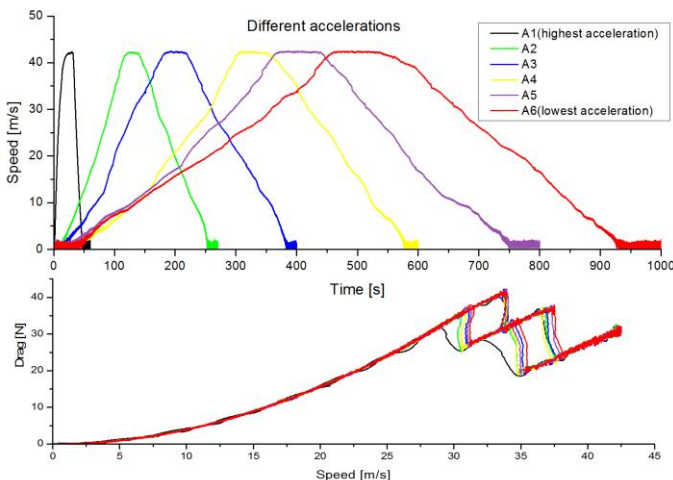


**Figure 44- Different accelerations, Drag - speed curve for six different speed gradients**

**Figure 45** shows a zoom in the critical area for the highest, A1 ( $1.33 \text{ m/s}^2$ ) and lowest acceleration, A6 ( $0.08\text{m/s}^2$ ). It is clear that acceleration have impact on the size of the hysteresis cycle. Higher acceleration increases the size of the cycle while low acceleration reduces it. This confirms to the results to the previous findings in the project thesis[3]. In this study the lowest acceleration

conducted was  $0.4\text{m/s}^2$  [3] and the present results, shown in **Figure 44**, were conducted for the lowest acceleration of  $0.08\text{m/s}^2$ . Comparing the result from the previous project thesis with the results in this study, a smaller hysteresis cycle can be seen in the present work. This is not surprising since the measurements were conducted with lower wind accelerations than the previous ones. The lowest acceleration did not eliminate the hysteresis phenomena, so the same assumption drawn from the previous results can be drawn from the present ones. It can be than speculatively said that if the acceleration was reduced even more at some point the hysteresis phenomena in the drag crisis process will be eliminated and explaining why static measurements do not show the hysteresis cycle.

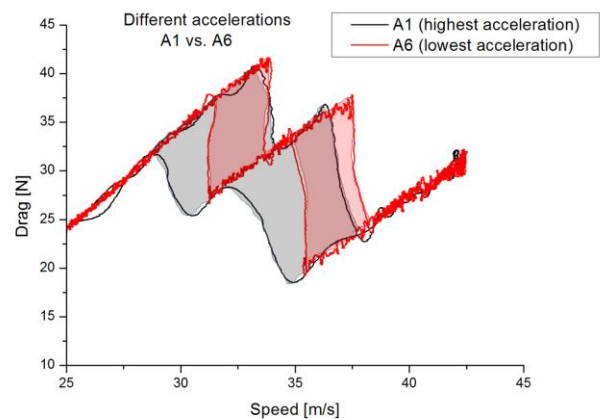


**Figure 45- Drag-speed curve for acceleration A1 and A6**

## G. SUITS, mannequin

In this section the results from the static drag measurements on the real size mannequin in a running posture are presented and discussed. The results will give a clear indication of how different suits are able to influence the drag acting on the model. The plots relative to the three suits developed by Adidas and the NTNU suit are presented in the same **Figure 46** and hereby described:

A1: Adidas suit with strips and dots placed on the outside surface. The strips are only placed on the front side of the suit.

A2: Adidas suit A1, but turned on the inside out, so that the configuration of the strips and dots are on the inside surface.

A3: Adidas suit without strips

NTNU: Modified underlayer strip developed at NTNU placed under Adidas suit A3.

From the acquired data for static measurements, the drag coefficient,  $C_D$  was plotted against speed. The results are in a speed range from 0 to 20 m/s. The results indicate that the strips have influence on the flow around the athlete's body. By using the underlayer strips placed under the fabric (NTNU), the results show that it is possible to reduce the drag coefficient,  $C_D$  with 6.5% by comparing the suit without strips (A1). By comparing the suit where the strips are placed on the outside surface (A1) with the suit where the strips are placed under the fabric (A2), the results shows clearly that it is beneficial to place strips on the inside surface since this configuration have the ability to achieve lower  $C_D$  values than for the strips placed on the outside surface. This confirms the results obtained for the different types of cylinders. By comparing the Adidas suit A2 with the suit developed at NTNU the results show that the composition of the strips is of great importance and must be consider for further work of optimization of low drag suit.

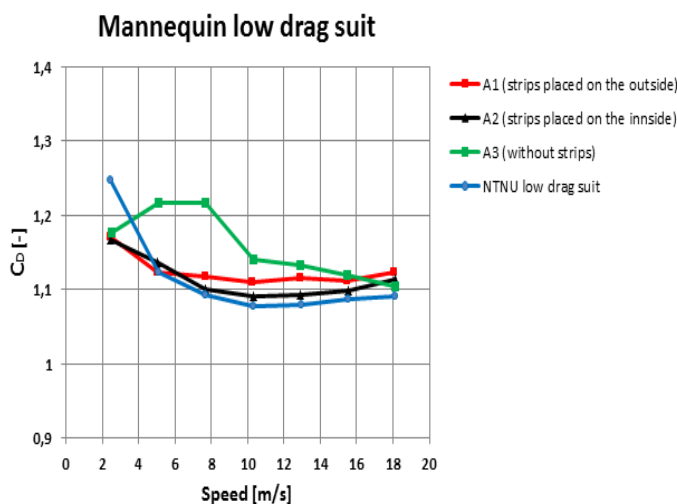


**Figure 46- Mannequin, A1, A2 and A3 low drag suits developed by Adidas. NTNU low drag suit developed by NTNU**

## VI. SUMMARY

The contour plots shown in **Figure 47 – Figure 56** show a graphic representation of the relationships between numbers of strips and speed relative to the drag coefficient,  $C_D$  in two dimensions. The results shown in the contour plot have already been discussed in detail in the previous section; this section will just give a summary and a basic guideline for further work of sports garment optimization.

The results in the contour are based on the dynamic time series for increasing wind speed. The variable in the X axes represent the speed range from 5-40m/s, where speeds (<5m/s) were removed because of the high uncertainties of drag computation at low speeds. The variable in the Y axes represent the number of strips, where 32, 16, 8 and without strips was plotted. The third variable Z shows the contour levels for the non-dimensional drag coefficient,  $C_D$ . The color mapping assigns the blue color to the minimum  $C_D$  value of the couture and the red color to the maximum  $C_D$  value and thus where the athletes experience the highest resistance in terms of drag. All the figures from the contour plot are hereby presented. In the discussion only low speeds (<15m/s) will be discussed.

**Figure 47** and **Figure 48** show the contour plots for the oval cylinder placed vertically with an angle of attack ( $\alpha$ ) of  $90^\circ$ . The plots clearly show that both fabrics can achieve low  $C_D$  values, however by using a smooth configuration, T3 with 16 strips it is possible to achieve lower drag coefficient,  $C_D$  than a rough surface configuration, T1.

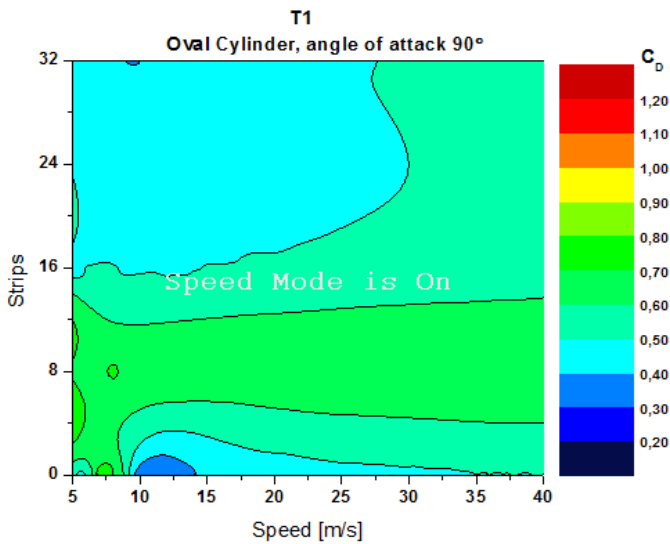


Figure 47 - Contour plot, oval cylinder angle of attack  $90^\circ$ , fabric T1

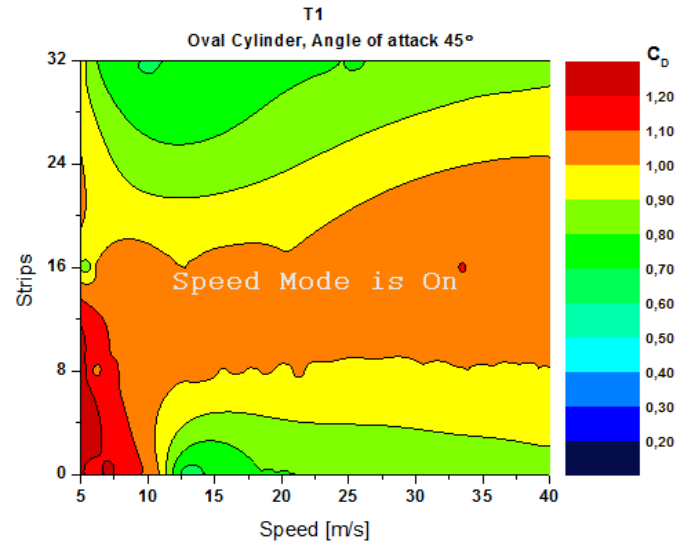


Figure 49- Contour plot, oval cylinder angle of attack  $45^\circ$ , fabric T1

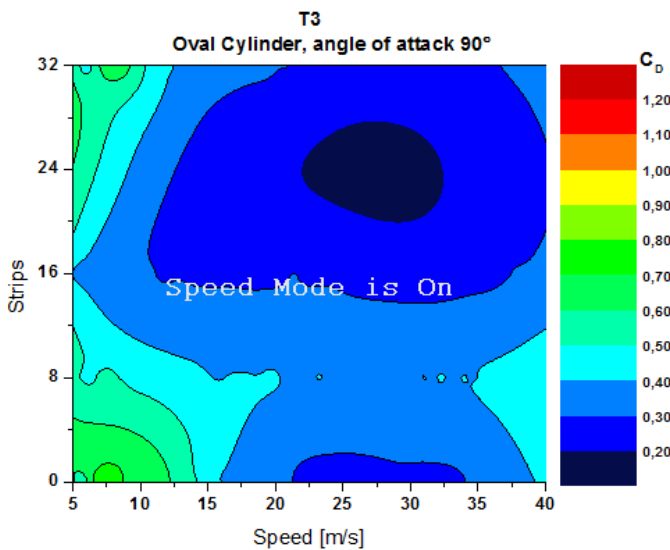


Figure 48- Contour plot, oval cylinder angle of attack  $90^\circ$ , fabric T3

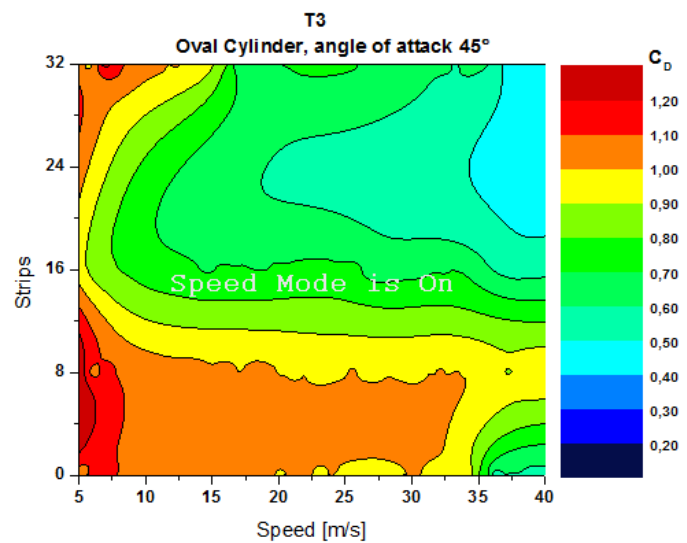


Figure 50- Contour plot, oval cylinder angle of attack  $45^\circ$ , fabric T3

Figure 49 and Figure 50 show the contour plots for the oval cylinder placed vertically with an angle of attack ( $\alpha$ ) of  $45^\circ$ . With respect to low speed the contour shows that it is beneficial to place 32 strips under rough fabric, T1 and for the smooth fabric, T3 16 strips is the best option to achieve low  $C_D$ .

Figure 51 and Figure 52 show the contour plots for the oval cylinder placed vertically with an angle of attack ( $\alpha$ ) of  $0^\circ$ . Both contour show that the drag coefficient,  $C_D$  is almost constant over the whole speed range and the values are almost the same wherever the textile is smooth or rough. Focusing on low speeds the contour shows that it is beneficial to use 32 strips placed under fabric, T1 for optimal drag reduction and for fabric, T3 8 strips.

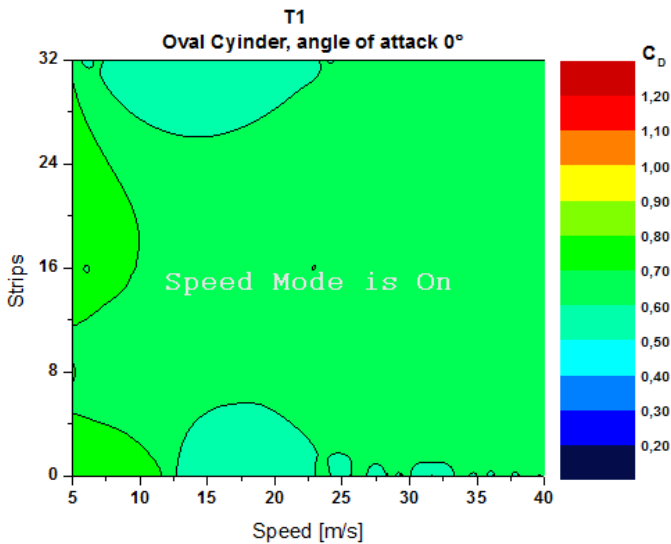


Figure 51- Contour plot, oval cylinder angle of attack  $0^\circ$ , fabric T1

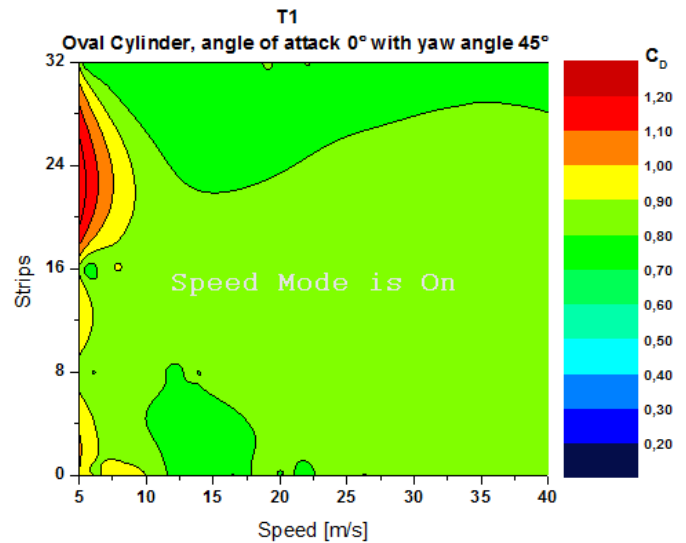


Figure 53- Contour plot, oval cylinder angle of attack  $0^\circ$  and sweep angle  $45^\circ$ , fabric T1

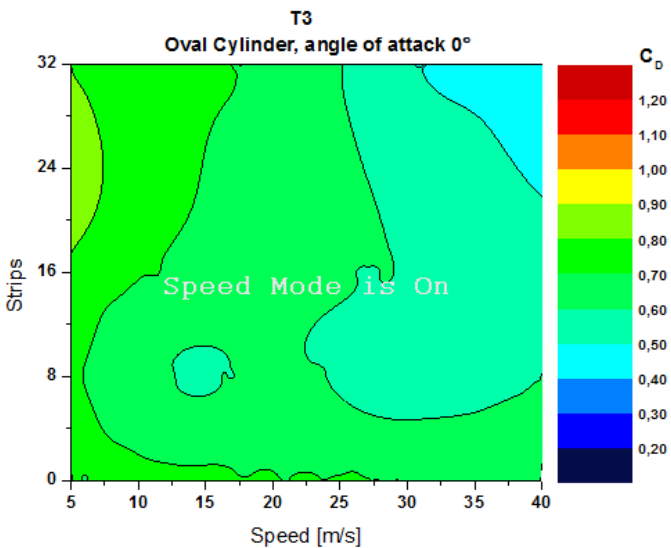


Figure 52- Contour plot, oval cylinder angle of attack  $0^\circ$ , fabric T3

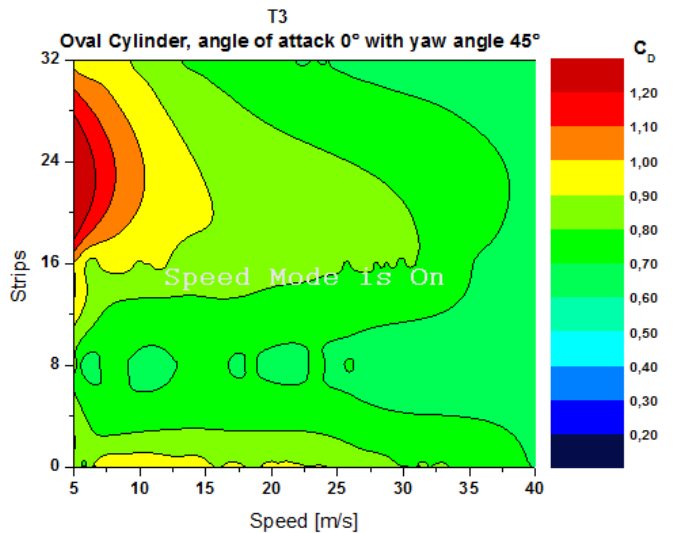


Figure 54- Contour plot, oval cylinder angle of attack  $0^\circ$  and sweep angle  $45^\circ$ , fabric T3

Figure 53 and Figure 54 show the contour plots for an angle of attack ( $\alpha$ ) of  $0^\circ$ , placed with a yaw angle ( $\lambda$ ) of  $45^\circ$ . In terms of drag reduction at low speeds will it be beneficial to place 32 strips under fabric T1. For fabric T3 will it be beneficial to place 8 or 16 strips.

Figure 55 and Figure 56 show the contour plots for the tapered cylinder. In terms of drag reduction at low speeds both fabric, T1 and T3 shows that it is beneficial to place 16 strips under the fabrics for maximum optimization.

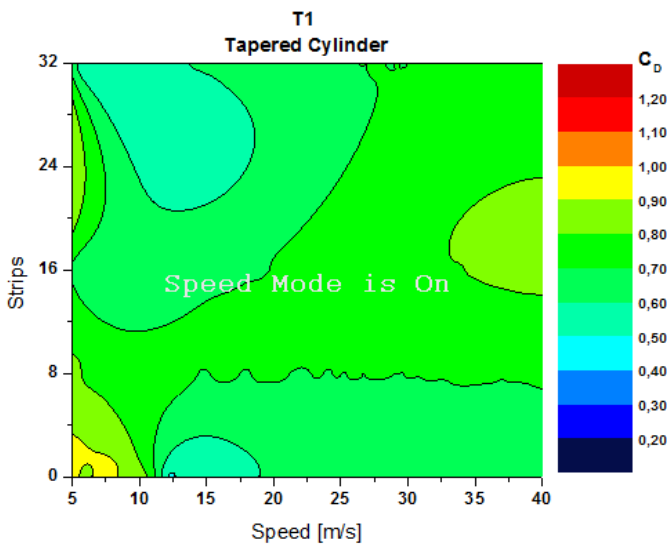


Figure 55- Contour plot, tapered cylinder, fabric T1

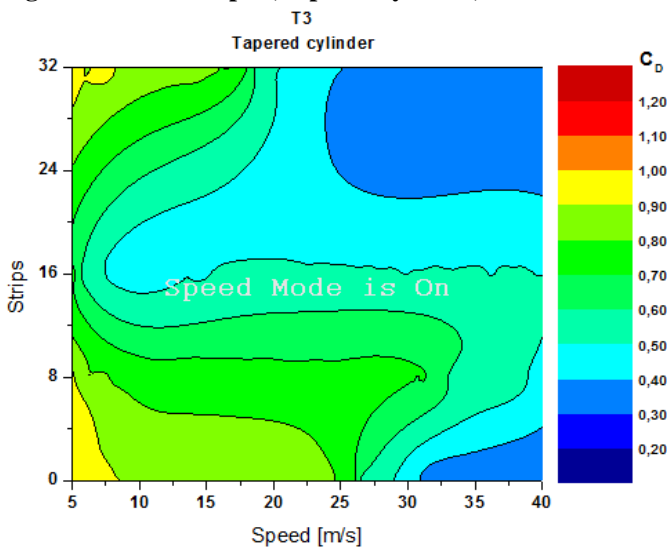


Figure 56- Contour plot, tapered cylinder, fabric T3

## VII. CONCLUSION

From this study many concluding marks can be drawn based on the experimental study of the drag optimization in sports garment for 100 m sprinting race. The results presented in this work makes it possible to take a closer step in the design optimization of the garment and also give the reader some basic guide lines for further work in design of low drag suits.

The underlayer strips representing the macrostructure of the fabric were compared with the fabric without the strips, where only the microstructure is present. Results clearly showed that the modified surface structure strips placed

under the fabrics have the ability to trigger the flow transition at low speed and with low  $C_D$  values on all the models tested (tapered, cylinder and oval cylinder with different angularity). This type of surface configuration have shown to be beneficial for running disciplines ( $<15\text{m/s}$ ), because it is possible to shift the transition to very low critical Reynolds numbers (speed) and with a consequent reduction in  $C_{D\text{MIN}}$  values.

Different angles of attack ( $\alpha$ ) on oval cylinders have been proven to have a huge influence on the flow transition. The results were in agreement with the theory.

The tapered shape have shown in the result to have the almost exactly the similar behavior as for the cylindrical cylinder tested in the previous project thesis.

The strips thickness and width showed to have no large impact on the drag coefficient,  $C_D$ , but a general trend was that the strips properties for the smallest thickness and width ( $1\text{mm}\times 1\text{mm}$ ) have the ability to achieve lower critical Reynolds numbers (speed) for both smooth and rough surface structure. The results also showed that it is important to consider the strips properties when a smooth surface structure is used, because the different strips properties have influence on the drag crisis area where the transition goes from laminar to turbulent, with the conclusion that the smooth fabrics are more sensitive in this area.

Strips placed under the fabric resulted to improve performances on all the models tested while strips placed on the outside did not show any benefit.

Hysteresis phenomena were found regardless the applied model used (except the oval cylinder placed in yaw angle of  $45^\circ$  where the hysteresis did not occurs) matching the results present in the literature. The hysteresis phenomena in the drag crisis process showed to be more sensitive for the smooth fabric structure than rough fabric structure which confirms with previous findings in the project thesis. The results also showed that with a rough fabric it is

possible to achieve lower critical Reynolds number for all applied models (cylinder, oval and tapered), than for smooth fabric. However with the right configuration of strips it is possible to achieve low critical Reynolds number and also to keep the  $C_D$  values low.

The results from the different accelerations test conducted showed that higher accelerations produce a larger hysteresis cycles than low acceleration.

The final outcome is that it is possible to develop a low drag suit with the knowledge on how the flow acts around different bluff bodies with different shapes, size and angularity and inclination. The mannequin tested wearing the custom designed suit showed that it is possible to achieve lower drag coefficient,  $C_D$  by using an under layer made of rubber strips. Comparing the results obtained for the custom designed suit with the results obtained for the Adidas designed suit (A2) a large improvement can be seen. Further improvements can be made rearranging the strips on the model and optimizing the distance and the size between them.

#### ACKNOWLEDGMENT

This paper is a concluding master thesis in civil engineering at Norwegian University of Science and Technology (NTNU). The study has been conducted throughout 21 weeks and involved literature research, experiments and analyzing of measurements. The master thesis has sponsored by Adidas and I have been very lucky to have the opportunity to be involved in researching of garment optimization for sprinting discipline.

I would like to give especially thank to Luca Oggiano for helpful guidelines, great support and encouragement during the whole semester. I will also like to thank my supervisor Lars Roar Sætran for all the helpful guidelines. Thanks also to Lars Morten Bardal for always being there for me if I needed help with the experiments. I would also like to thank Arnt Egil Kostad for constructing necessary equipment and rigging in the wind tunnel.

#### REFERENCES

1. Heck, A. and T. Ellermeijer, *Giving students the run of sprinting models*, 2009, AMSTEL Institute: Amsterdam.
2. Cimbala, J.M. and Y.A. Cengel, *Essentials of Fluid Mechanics*, ed. M.-. Hill. 2008, NY - USA.
3. Sæter, C., *Experimental investigation on cylinders with tailored surface structure using dynamic and static force measurements*, in *Department of Energy and Process Engineering 2012*, NTNU: Trondheim - Norway.
4. Zdravkovich, M.M., *Flow Around Circular Cylinder - Applications*, ed. O.U. Press. Vol. 2. 1997, Oxford - England.
5. Zdravkovich, M.M., *Flow around circular cylinders - Applications*, ed. O.U. Press. Vol. 1. 1997, Oxford - England.
6. Wieselsberger, C., *Neuere Feststellungen über die Gesetze des Fliissigkeits- und Luftwiderstands*. *Physiscs*, 1921. **2**(22): p. 321-328.
7. Schewe, G., *On the force fluctuations acting on a circular cylinder in crossflow from subcritical up to transcritical Reynolds numbers*. *Journal of fluid mechanics*, 1981.
8. Schewe, G., *Sensitivity of transition phenomena to small perturbations in flow round a circular cylinder*. *Journal of fluid mechanics*, 1986. **172**: p. 33-46.
9. Zdravkovich, M.M., *Conceptual overview of laminar and turbulent flows past smooth and rough circular cylinders*. *Journal of Wind Engineering and Industrial Aerodynamics*, 1990. **33**: p. 53-62.
10. Achenbach, E., *Influence of surface roughness on the cross-flow around a circular cylinder*. *Journal of Fluid Mechanics*, 1970. **46**(2): p. 321-335.
11. Bearman, P.W. and J.K. Harvey, *Control of Circular Cylinder flow by the use*

- of dimples. *AIAA-Journal*, 1993. **31**(10): p. 1753–1756.
12. Achenbach, E., *The effect of surface roughness on the heat transfer from a circular cylinder to the cross flow of air. International Journal of Heat and Mass Transfer*, 1977. **20**(5): p. 359–369.
  13. MacDonald, R., *Aerodynamic Garment for improved athletic Performance and Method Manufacture*, NIKE, Editor 2002: USA.
  14. Brownlie, L. and C.R. Kyle, *Evidence that skin suits affect long track speed skating performance. Procedia Engineering - ISEA2012*, 2012. **34**: p. 26-31.
  15. Wieland M, H.P., Hotz W, Textor M, Keller BA, and Spencer ND, *Wavelength-dependent measurement and evaluation of surface topographies: application of new concept of window roughness and surface transfer function. Wear*, 2000. **237**, 2000: p. 231-252.
  16. Bardal, L.M., *Aerodynamic properties of textiles*, in *Department of Energy and Process Engineering 2010*, NTNU: Trondheim - Norway.
  17. Metha, R.D. and J.M. Phallis, *Tennis ball aerodynamics and dynamics*, in *Biomedical Engineering Principles in Sports*. 2004, Kluwer Academic/Plenum Publishers. p. 99-123.
  18. Hoerner, S.F., *Fluid dynamic drag*. 1965, New York - USA: Hoerner S. F.
  19. Brownlie, L., *Aerodynamic characteristics of sports apparel*, in *School of Kinesiology 1992*, Simon Fraser University: Burnaby BC.
  20. Brownlie, L., et al., *Influence of apparel on aerodynamic drag in running. The Annals of physiological Anthropology*, 1987. **6**(3): p. 133-143.
  21. Oggiano, L. and L. Sætran, *Effect of different skin suits on speed skating performances. Computer science in sports*, 2008. **3**: p. 139–144.
  22. Oggiano, L., et al., *Reducing the athlete's aerodynamical resistance. Journal of computational and applied mechanics*, 2007. **8**(2): p. 163–173.
  23. Chowdhury, H., et al., *Design and methodology for evaluating aerodynamic characteristics of sports textiles. Sports Technology*, 2009. **2**(3-4): p. 81–86.
  24. Grieve, D.W., *Gait Patterns and Speed of Walking. Bio-medical Engineering*, 1986.
  25. Oggiano, L. and L. Sætran, *Experimental analysis on parameters affecting drag force on athletes. The impact of Technology on Sport*, 2009. **3**: p. 383-389.
  26. Wang.H.F, Z.J., Mi.J, *Effects of aspect ratio on the drag of wall-mounted finite-length cylinder in subcritical and critical regimes. Journal of fluid mechanics*, 2012.
  27. Shakin.A, H.S., *Aspect Ratio Effects on the Drag coefficient of a Cylinder*. 2011.
  28. Bosch.H.R, G.R.M., *Wind tunnel experimental investigation on tapered cylinders for highway support structure. Wind engineering*, 2001.
  29. Konopov I, O.L., Chinga-Carrasco G, Troynikov O, Sætran L, and Alma F, *Aerodynamics and comfort characteristics of double layer knitted fabric assembly for high speed winter sports. Procedia Engineering*, 2010. **2**(2), 2010: p. 2837-2843.
  30. A. D`Auteuil, G.L.L., S.J.Zan, *Relevance of similitude parameters for drag reduction in sport aerodynamic. Procedia Engineering ISEA 2010*, 2010: p. 2393-2398.
  31. Sykes, K., *Technique and observation of angular gait patterns in running. Journal of Sport Medicine*, 1975. **9**(4): p. 181-186.
  32. Schewe, G., *Reynolds-number effects in flow around more-or-less bluff bodies. Journal of fluid mechanics*, 2001.
  33. Yang, Z., et al., *An Experimental Investigation on Aerodynamic Hysteresis of*

*a Low-Reynolds Number Airfoil, in 46th AIAA Aerospace Sciences Meeting and Exhibit 2008: Reno, Nevada.*

34. Science, E., *ESDU-74031 Int. L+D, London. 1987.*

35. Schewe, G., *On the force fluctuations acting on a circular cylinder in crossflow from subcritical up to transcritical Reynolds numbers. Journal of fluid mechanics, 1983. 133: p. 265-285.*